Author's personal copy

Crude oil-induced cardiotoxicity in fishes

Edward M. Mager[a] **and Christina Pasparakis**[b], [a] Department of Biological Sciences, Advanced Environmental Research Institute, University of North Texas, Denton, TX, United States; and [b] Department of Environmental Toxicology, University of California, Bodega Marine Laboratory, Bodega Bay, CA, United States

© 2024 Elsevier Inc. All rights are reserved, including those for text and data mining, AI training, and similar technologies.

Key points

- Crude oil is comprised of thousands of chemicals, among which polycyclic aromatic hydrocarbons represent the putative principal components driving cardiotoxicity
- Narcosis, aryl hydrocarbon receptor (AhR) dependent and AhR independent pathways represent the three predominant hypotheses for mechanisms of crude oil cardiotoxicity
- The cardiotoxic crude oil phenotype in early life stage fishes is characterized by a syndrome of morphological and functional effects, with pericardial and yolk sac edema representing the most pronounced and commonly-reported form of injury
- Mounting functional and molecular analyses support targeted disruptions to excitation-contraction coupling as an underlying mechanism of crude oil cardiotoxicity
- Implications of crude oil induced cardiac injury to swimming performance and thermal/hypoxia tolerances are also addressed

Abstract

Crude oil spills in the aquatic environment, particularly large-scale disasters like the Deepwater Horizon and Exxon Valdez events, pose significant threats to the health and survival of resident biota. Accumulating evidence supports the developing heart as a primary target of crude oil toxicity in fishes. This chapter summarizes the predominant morphological, functional and molecular alterations in fish arising from crude oil exposures, mainly during the early life stages, as well as the prevailing hypotheses for the underlying mechanisms of cardiotoxicity. Implications of acute and chronic/latent cardiac effects in later life stage fishes related to aerobic performance and thermal/hypoxia tolerances are also explored.

Author's personal copy

Teaching slide

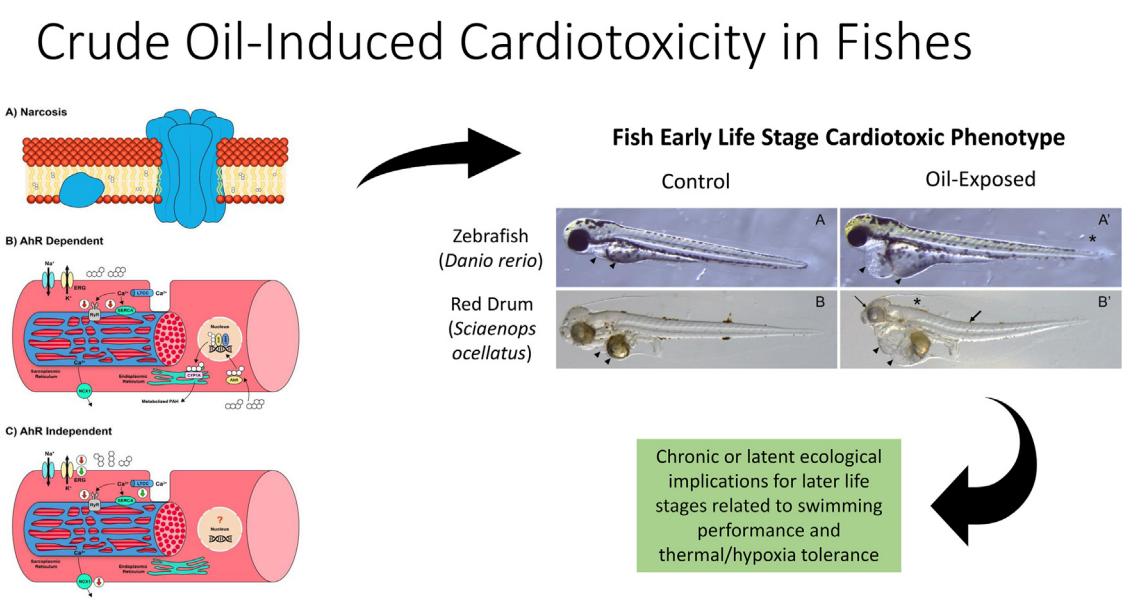

Introduction

High demand for petroleum-based products continues to drive the exploration, extraction, transport and processing of crude oil from the environment. Yet, encouraging historical trends have demonstrated persistent global declines in the number of oil spills and overall volumes released (Eckle et al., 2012). While these declines have been driven mainly by reductions in tanker spills, pipeline and storage/refinery spills have increased, likely shifting greater threats to freshwater communities (Eckle et al., 2012). Despite these generally positive trends, periodic catastrophic events, such as the Macondo well blowout that led to the Deepwater Horizon (DWH) oil spill in 2010, can have devastating and long-lasting effects on resident biota (Barron et al., 2020). With respect to fishes, as we will see, the early life stages (ELS) are typically the most sensitive to crude oil exposure. As described in greater detail later, the phenotype of crude oil exposed ELS fishes is typically characterized by functional and morphological alterations related to the developing heart, including reduced heart rate (i.e., bradycardia), arrhythmias and pericardial and yolk sac edema. Moreover, the suite of effects that contribute to the phenotype is consistently observed across geologically distinct sources of crude oil (Jung et al., 2013). While these effects likely contribute to, if not outright cause, acute mortality at sufficiently high concentrations, more subtle cardiac defects arising from lower concentrations may impart persistent or latent effects on later life stages. Considering the role of the heart in sustaining ecologically important behaviors with high aerobic demand, such as migration, foraging and predator-prey interactions, such subtle effects could lead to additional delayed mortalities as a result of reduced swimming capacity (Plaut, 2001). Additionally, it is reasonable to expect that crude oil induced cardiac impairments might also reduce fish thermal and hypoxia tolerances.

This chapter aims to summarize what is currently known regarding the cardiotoxic responses of fishes to crude oil exposure. To set the stage, we begin with a description of crude oil constituents and weathering effects followed by an overview of the three main hypotheses for describing the underlying mechanism(s) of cardiotoxicity. We then review the predominant morphological, functional and molecular responses to crude oil exposure related to cardiotoxicity, focusing on ELS fishes. Where useful for providing additional insight, studies of individual polycyclic aromatic hydrocarbons (PAHs) are included. We then conclude by examining the potential implications of acute and chronic/latent sublethal cardiac effects in juvenile and adult fishes, specifically related to aerobic swimming capacity and thermal/hypoxia tolerance. As will likely become apparent, difficulties in drawing comparisons and overarching conclusions arise due to inconsistencies in species and life stages used, as well as in specific methodological approaches, such as exposure initiation and duration, oil type and weathering state, mixing methods, use of dispersants, and the constituent chemicals/units used for characterizing exposures. Finally, while both biotic (e.g., competition, predation) and abiotic (e.g., temperature, ultraviolet (UV) light) factors may dramatically influence crude oil toxicity, their specific mechanistic roles in mediating cardiotoxic effects remain largely uncharacterized and thus will not be specifically addressed in this chapter.

Author's personal copy

Crude oil composition

Crude oils are comprised of extremely complex mixtures of hundreds of thousands of chemicals, including both polar and nonpolar compounds. While the specific identities of the vast majority of these chemicals remain unknown, the main classes of compounds and many of their individual constituents have been at least broadly characterized. The main classes of constituents include the linear/branched alkanes, cycloalkanes, monocyclic and polycyclic aromatic hydrocarbons (PAHs), heterocyclic compounds, asphaltenes and resins. Heterocyclics are similar in structure to PAHs but contain a heteroatom (any atom other than carbon or hydrogen) in place of a carbon within the cyclic parent structure (**Fig. 1**). These are also commonly referred to as NSO compounds, owing to the prevalence of nitrogen (e.g., carbazole), sulfur (e.g., dibenzothiophene), or oxygen (e.g., dibenzofuran) atoms serving in this role. Although these fall under the more general category of polycyclic aromatic compounds (PACs), they are often included in measurements of total PAHs; hence, we will maintain the typical standard within the ecotoxicology literature of including heterocyclics as PAHs to avoid confusion. Again, however, most of the specific compounds in crude oil remain unidentified and this fraction has historically been referred to simply as the unresolved complex mixture (UCM; although see Farrington and Quinn (2015) for the origin and clarification on the use of this term). Finally, crude oils also contain trace metals such as iron, nickel and copper, although the bioavailability and toxicity of such contaminants remain largely unknown.

With respect to crude oil exposures to fishes, most work has focused on PAHs as the likely main drivers of toxicity. These compounds typically comprise only a relatively small fraction of crude oil (0.2 to >7%) (National Research Council Committee on Oil in the Sea: Inputs, Fates, and Effects, 2003), as exemplified by the estimated 3.9% of PAHs by weight measured within DWH crude oil (Reddy et al., 2012). PAHs are defined by having two or more fused benzene rings that can be modified by the addition of various moieties along the carbon backbone (**Fig. 1**). Common modifications to the parent PAH include alkylation and addition of oxygen species (e.g., hydroxylation, quinone formation), each of which can have significant ramifications for the toxicity of individual compounds (e.g., Rhodes et al., 2005). Unfortunately, current analytical techniques and equipment are unable to routinely distinguish among many substituted homologs, for example those differing only by alkyl chain position, length or branching, and thus precludes our ability to specifically define the modified constituents, their concentrations and relative proportions within crude oil samples.

To complicate matters further, the chemical composition of crude oil can vary depending on its geological source and state of weathering. For example, the physical and chemical characteristics of oils released during the Exxon Valdez oil spill (EVOS) and DWH spill differ considerably, with the former considered a heavier, sour oil (due to a higher proportion of aromatic and sulfur-rich compounds) and the latter a lighter, sweet oil. Weathering, on the other hand, is a complex process of oil transformation involving dilution, evaporation of the lower molecular weight components, photo-oxidation and microbial degradation that alters the chemical structure, concentration and relative proportion of crude oil constituents. Specifically, weathering causes the loss of the volatile monocyclic compounds (benzene, toluene, ethylbenzene and xylenes (BTEX)) and bicyclic naphthalenes, thus concentrating the heavier molecular weight components that remain, including PAHs with ≥3 rings. Such differences in crude oil composition have important implications for toxicity, as will be addressed later. However, measuring the concentrations of individual

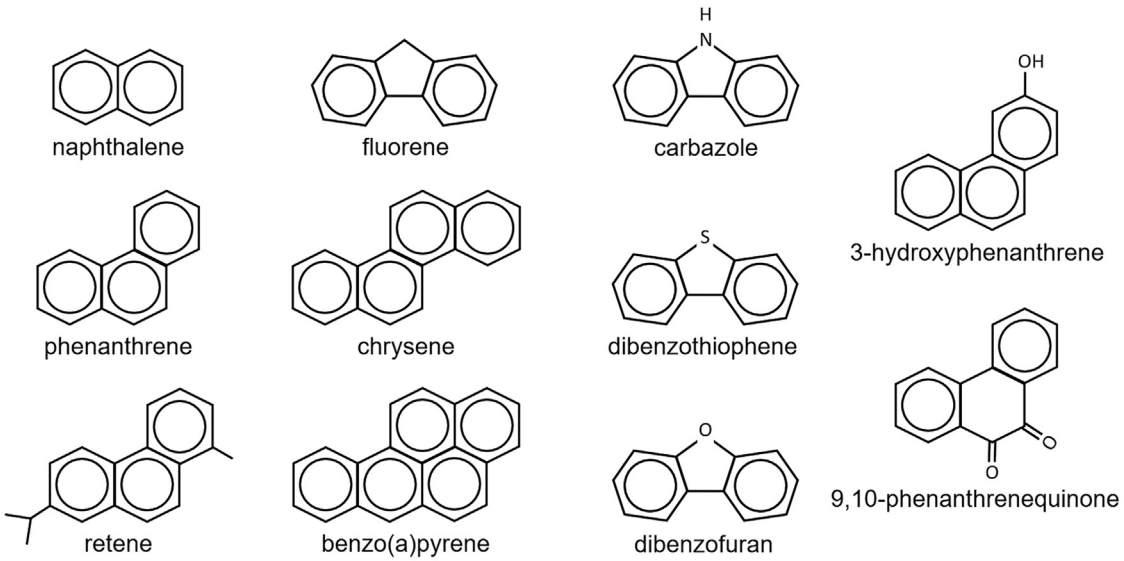

Fig. 1 Example illustrations of polycyclic aromatic compound (PAC) constituents within crude oil. The first two columns provide examples of 2- to 5-ring polycyclic aromatic hydrocarbons (PAHs), including an example of a 4-carbon (C4) alkylated homolog of phenanthrene, retene. The third column illustrates examples of heterocyclic PACs for each of the major heteroatoms (i.e., nitrogen, sulfur and oxygen; NSO compounds) and the fourth column provides examples of phenanthrene moieties modified by the addition of oxygen. Such oxygenated products can arise from photochemical oxidation, microbial transformation or endogenous Phase I metabolism of the parent PAH.

Author's personal copy

BTEX and PAH constituents can impose significant financial burdens. Thus, there is a range of select PAHs that researchers choose to measure, typically ranging from the USEPA's 16 priority pollutant PAHs to the more expansive 40–50 PAHs commonly reported in studies following the DWH spill (see for example Incardona et al., 2014). The individual PAH concentrations are simply added together and reported in units of sum or total PAHs (i.e., ΣPAHs or tPAHs, respectively). Still others report measurements of total petroleum hydrocarbons (TPH), which as the designation implies, considers hundreds of chemicals including alkanes and PAHs, among others, but typically provides no information on individual constituents. Again, such inconsistencies in reporting exposure concentrations present obvious challenges for cross-study comparisons.

Mechanisms of cardiotoxicity

From the outset, it should be noted that while great strides have been made in the field of crude oil ecotoxicology largely following the EVOS and DWH events, much still remains to be learned regarding the mechanisms of toxicity resulting from crude oil exposures to fishes, including that specifically related to the heart. Indeed, there remains considerable debate as to the likely primary cause(s) of cardiotoxicity. The prevailing hypotheses are represented by a nonspecific narcosis-based model and two receptor-based models, one that is mediated by the aryl hydrocarbon receptor (AhR) and another that acts independently of the AhR and instead relies on cardiac ion channels as the proposed receptors (**Fig. 2**). This chapter will consider each of these in turn; however, the focus will remain solely on summarizing the central tenets of each as there are other excellent recent reviews that highlight and argue the key points of debate (see for example: Hodson, 2017; Incardona, 2017; Meador, 2021; Meador and Nahrgang, 2019).

Narcosis

The earliest school of thought contends that the toxicity of crude oil to aquatic organisms is mediated primarily through nonspecific narcotic mechanisms, otherwise known as baseline toxicity. The basic premise is based on the target lipid model (TLM) of toxicity that relates a chemical's acute toxicity (as median lethal concentration (LC50)) to its respective octanol–water partition coefficient (K_{ow}), a unitless measure of a chemical's lipid versus water solubility (values >1 indicate greater lipophilicity) (Di Toro and McGrath, 2000). This approach was later applied to estimate the toxic potential (i.e., solubility to toxicity ratio) of complex oil water mixtures (Di Toro et al., 2007) and assess the toxicity of select petroleum hydrocarbons (e.g., McGrath et al., 2018). Essentially, the model proposes that organic molecules accumulate within biological lipids, most functionally important in terms of acute toxicity, the lipid bilayer of cellular membranes (**Fig. 2**A). At sufficient concentrations, such chemicals are thought to negatively affect the integrity and fluidity of these membranes, ultimately leading to widespread cell death and organismal mortality. The potential toxic mechanism here is a disruption in ion homeostasis due to a nonspecific disruption of biological membranes that alters the function of membrane-bound proteins, including ion channels (Sikkema et al., 1995). In terms of cardiotoxicity specifically, ionic imbalances of this nature would obviously impair the normal contractile properties of the heart that rely on regulated ionic fluxes, mainly those of Ca^{2+}, K^{+} and Na^{+}. The TLM predicts that low molecular weight PAHs and volatile BTEXs within crude oil are the more harmful components in this regard (Di Toro et al., 2007), which as we will see is contrary to the receptor-based hypotheses of cardiotoxicity that contend that higher molecular weight PAHs, particularly the tricyclic PAHs, are primarily responsible for cardiotoxicity arising from crude oil exposure.

AhR dependent pathway

The AhR is a cytosolic ligand-activated transcription factor that regulates a rather large and diverse array of genes. The receptor is activated by both synthetic and naturally occurring chemicals, although the search for an endogenous high-affinity ligand remains elusive. Nevertheless, it is now widely thought to serve two general roles, one as a sensor of xenobiotic chemicals and another as a contributor to the proper functioning of various organ systems by regulating different aspects of cell maintenance, differentiation, proliferation and migration (Mulero-Navarro and Fernandez-Salguero, 2016). In its inactivated state, AhR is bound by a number of chaperones, including AhR interacting protein (AIP) and a dimer of heat shock protein 90 (HSP90), along with other proteins that aid in maintaining proper structure and preventing premature binding to its initial target, the AhR nuclear translocator (ARNT). Once bound to a ligand, the AIP disassociates thereby exposing the nuclear localization sequence and facilitating translocation to the nucleus where the ligand-bound AhR then dimerizes with the ARNT. This complex then binds DNA at xenobiotic response elements (XRE) to activate transcription (Denison and Nagy, 2003). The transcription targets of this process include members of a gene battery encoding Phase I and Phase II metabolic enzymes. Key among these are the cytochrome P450 (CYP) superfamily of enzymes, most notably CYP1A which is involved in the Phase I conversion of highly hydrophobic xenobiotics (e.g., organochlorines and PAHs) to more reactive metabolite intermediates. Phase II enzymes, such as glutathione S-transferase (GST), then add hydrophilic moieties to enhance solubility of the metabolites and facilitate excretion through the urine or bile (Köhle and Bock, 2007).

While the formation of reactive metabolites from Phase I metabolism represents an important potential source of general toxicity, it is the alteration in the expression of genes elicited by the AhR outside this gene battery of Phase I/II enzymes that likely explains at least a portion of the observed cardiac-specific toxicity of crude oil (**Fig. 2**B). For example, genes encoding the sarcoplasmic reticulum calcium ATPase (SERCA) pump and the ryanodine receptor 2 (RyR) have been shown to be downregulated, likely

Author's personal copy

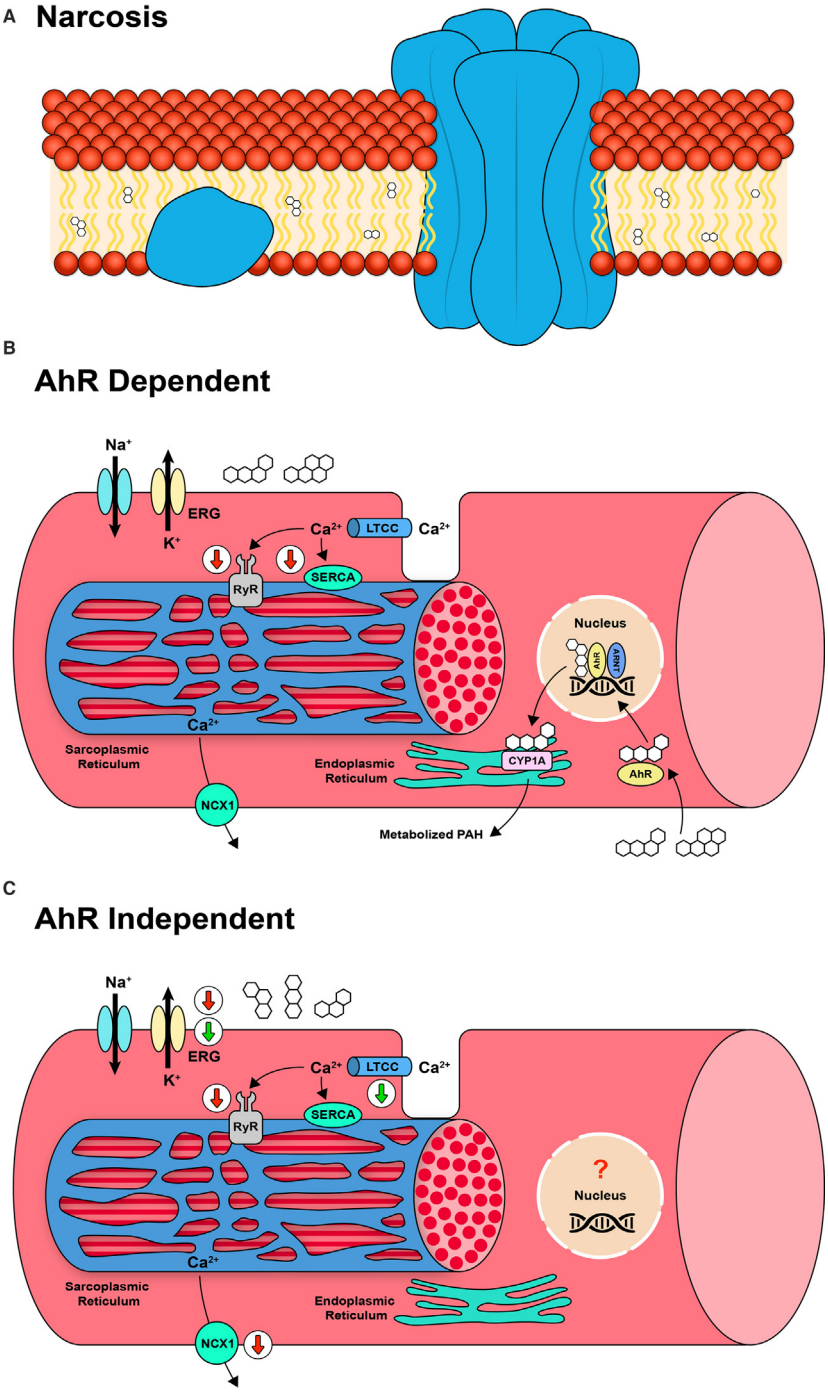

Fig. 2 Graphical summary of the three main mechanistic hypotheses for crude oil induced cardiotoxicity in fishes. The narcosis model (A) proposes that low molecular weight organic molecules, including polycyclic aromatic hydrocarbons (PAHs) and volatile BTEX (benzene, toluene, ethylbenzene and xylenes) compounds accumulate within the lipid bilayer of cellular membranes, negatively impacting their integrity and fluidity in a non-specific manner. As a result, the functions of membrane-bound proteins, including ion channels involved in cardiomyocyte contraction, are impaired, ultimately leading to widespread cell death and organismal mortality. In the aryl hydrocarbon receptor (AhR) dependent pathway (B), higher molecular weight PAHs first bind with the intracellular AhR and the complex is then transported to the nucleus where it binds with the AhR nuclear translocator (ARNT). This complex then binds DNA at xenobiotic response elements (XRE) to activate transcription of genes involved in xenobiotic metabolism, such as cytochrome P450 (CYP1A) that may produce more toxic metabolites than the parent compound, or alter other gene expression pathways (not shown) that downregulate genes involved in Ca^{2+} cycling (among others), namely the ryanodine receptor 2 (RyR) and the sarcoplasmic reticulum calcium ATPase 2 (SERCA) pump (red arrows). Finally, in the AhR independent pathway (C) tricyclic PAHs directly block Ca^{2+} influx (I_{Ca}) and K^{+} efflux (I_{Kr}) involved in excitation-contraction coupling through inhibition of the L-type calcium channel (LTCC) and the ether-a-go-go related gene (ERG), respectively (green arrows). Subsequent altered expression of various genes, such as ERG, RyR and sodium/calcium exchanger 1 (NCX1), among others, may also contribute to this pathway through currently unknown mechanisms (red arrows). (B) and (C) Adapted from (Incardona, 2017).

Author's personal copy

due to prolonged AhR activation, in response to exposure to individual high molecular weight PAHs, including benz(a)anthracene and benzo(a)pyrene (e.g., Jayasundara et al., 2015). Both of these targets (i.e., SERCA and RyR) are integral to proper calcium cycling within cardiomyocytes and are thus critical for regulating sarcomere contractility. Moreover, bone morphometric protein 4 (BMP4), an important signal in early heart development, was also shown to decrease in expression in response to benzo(a)pyrene exposure (Jayasundara et al., 2015).

It should be noted that while higher molecular weight PAHs such as those just described are potent AhR activators they also tend to be poorly concentrated within crude oil exposures, often falling below detection limits. By contrast, the parent PAHs most abundant in crude oil, such as naphthalenes and phenanthrenes, are weak AhR agonists (Barron et al., 2004). Interestingly, however, it seems that the alkylated homologs of tricyclic PAHs, which are typically more abundant in crude oil than their parent compounds, may serve as more potent AhR ligands than their parent counterparts and thus contribute more heavily to the AhR dependent pathway. A notable caveat is that this proposition is based largely on studies of retene, a C4 alkylated form of phenanthrene that is typically found at low concentrations in crude oil (Incardona, 2017); hence, a clearer determination as to the contribution of alkylated tricyclics to the AhR dependent pathway warrants additional study with more representative alkylated homologs.

AhR independent pathway

Generally speaking, the AhR independent pathway of crude oil cardiotoxicity involves similar outcomes as the AhR dependent pathway in terms of disrupted ion fluxes impacting myocyte contractility. The major differences between these two pathways are the primary PAH compounds driving toxicity and the specific modes of action. As alluded to previously, the AhR dependent pathway attributes toxicity to the higher molecular weight PAHs ($\geq$4 rings and potentially alkylated 3-ring compounds), whereas the AhR independent pathway attributes toxicity to the parent 3-ring PAHs. While the supporting evidence will be presented in greater detail in the sections that follow, the basic premise of the AhR independent pathway is that both Ca^{2+} and K^{+} fluxes/intracellular cycling are disrupted within cardiomyocytes by direct interactions between tricyclic PAHs and the channels/transporters for these ionic species (**Fig. 2**C). Pioneering work in this area by Incardona and colleagues provided the initial evidence in support of this pathway. Exposure of embryonic zebrafish (*Danio rerio*) to the 3-ring PAHs phenanthrene or dibenzothiophene produced a phenotype of cardiac arrhythmias characterized by blocked atrioventricular conduction. This was identical to the phenotype produced by loss-of-function mutants or pharmacological blockade of the ether-a-go-go related gene (ERG) that encodes a K^{+} channel involved in the propagation of cardiac action potentials. Notably, the effect was exacerbated by knockdown of AhR isoforms or CYP1A, supporting an AhR-independent mechanism of toxicity (Incardona et al., 2005). Subsequent altered expression of these ionoregulatory genes and others through currently unknown mechanisms may also contribute to this AhR independent pathway (Incardona, 2017).

More recently, additional functional and molecular evidence has emerged supporting alterations to proper excitation–contraction (EC) coupling in developing cardiomyocytes as a likely mechanism for crude-oil induced cardiotoxicity. Here again the SERCA pump and RyR are believed to play key roles in altered Ca^{2+} cycling in addition to ERG and its function in cellular K^{+} flux. The process of EC coupling by myocytes is initiated by an action potential generated by the opening of voltage-gated Na^{+} channels. Subsequently, L-type Ca^{2+} channels (LTCC) open to permit extracellular Ca^{2+} to enter, followed by an internal release of Ca^{2+} from the sarcoplasmic reticulum (SR) via the RyR. The resultant transient increase in cytosolic Ca^{2+} promotes the uncovering of tropomyosin-blocked myosin binding sites along the actin filaments within sarcomeres, thereby activating cardiomyocyte contraction. During the relaxation phase, intracellular Ca^{2+} ions are restored to baseline by returning Ca^{2+} to the SR via SERCA and exporting Ca^{2+} from the cell by way of the sodium/calcium exchanger 1 (NCX1). To restore the membrane potential for the next cycle, K^{+} exits the cell through voltage-gated channels, such as ERG. Although direct interaction of PAHs with these molecular targets is still awaiting confirmation, recent electrophysiological studies provide strong evidence in support of tricyclic PAHs impairing the function of those specifically involved in Ca^{2+} and K^{+} cycling, namely SERCA2, RyR2 and ERG (see **Functional effects** below).

Morphological effects

Considering the overt teratogenic effects that were largely the focus of early studies following the EVOS, and more recently following the DWH spill, a summary of morphological effects is provided first. By far, most of these studies center on effects during the ELSs as they tend to be the most sensitive life stages to toxicant exposure (**Table 1**). The characteristic cardiotoxic phenotype is represented by a suite of gross morphological defects defined by various alterations to normal heart development (described in more detail below), pericardial and yolk sac edema, various fin and craniofacial malformations and distortion of the body axis (spinal curvature), with pericardial and yolk sac edema representing the most pronounced and commonly-reported form of injury (**Fig. 3**). The suite of effects is similar to that produced by exposure to dioxins and polychlorinated biphenyls (PCBs), which led to the term "blue sac disease" (BSD; sometimes also referred to in the oil/PAH literature) owing to the opalescent appearance of yolk sacs in exposed salmonid larvae (e.g., Spitsbergen et al., 1991). In terms of the heart itself, it is useful to first review what is known regarding the process of normal cardiac development before detailing alterations due to crude oil exposure. To be concise, only those developmental steps with clear and direct links to cardiotoxicity will be explored.

Author's personal copy

Table 1 Summary of morphological effects of crude oil exposure in fish.

Species	*Oil type*	*Oil prep*	*Life stage/ age at measurement*	*Temp (°C)*	*Oil exposure duration (Days)*	*Process impacted or endpoint*	*Direction of change*	*Lowest effect concentration (μg/L)*	*No effect concentration (μg/L)*	*References*	*Notes*
Inland Silverside (*Menidia beryllina*)	DWH/leaking well riser by BP	WAF/CEWAF	Embryo/ Larva	21	3	Morphological abnormalities	↑	Oil/9500 = 44.18; Oil/9527 = 217.26 $\sum PAH_{47}$	Oil = 24.08 $\sum PAH_{47}$	Adeyemo et al. (2015)	Included: head malformation, pericardial edema and curvature of body Corexit 9500 & 9527 added to oil preparations
Atlantic Cod (*Gadus morhua*)	Troll field in the North Sea crude oil	Heated and HPLC pumped	Embryo/ Larva	7	3	Craniofacial malformations; spinal curvature	↑	50 $\sum PAH_{61}$	13 $\sum PAH_{61}$	Aranguren-Abadía et al. (2022)	Significant effects on spinal curvature with UV co-exposure only
Atlantic Cod (*Gadus morhua*)	Troll field in the North Sea crude oil	Heated and HPLC pumped	Embryo/ Larva	7	3	Ventricle diastolic (D) area; Ventricle systolic (S) area	↓	Ventricle D area- 200; Ventricle S area- 3 $\sum PAH_{61}$	Ventricle D area- 50 $\sum PAH_{61}$	Aranguren-Abadía et al. (2022)	Ventricle D area intensified with UV co-exposure
Atlantic Cod (*Gadus morhua*)	Troll field in the North Sea crude oil	Heated and HPLC pumped	Embryo/ Larva	7	3	Fractional Shortening (FS)	↓	FS- 3 $\sum PAH_{61}$	–	Aranguren-Abadía et al. (2022)	FS intensified with UV co-exposure
Japanese Medaka (*Oryzias latipes*)	Pyrene and methylpyrene	Sediment exposures	Embryo/ Larva	26	8	Developmental abnormalities	↑	–	–	Barjhoux et al. (2014)	Abnormalities included cardio-vascular, spinal, craniofacial, and pericardial edema
Zebrafish (*Danio rerio*)	Retene	Diluted in water	Embryo/ Larva	27	14	Pericardial edema	↑	EC50 = 144 hpf- 554; 240 hpf- 445	–	Billiard et al. (1999)	
Rainbow Trout (*Oncorhynchus mykiss*)	Retene	Diluted in water	Embryo/ Larva	7–11	42	Pericardial edema	↑	180	100	Billiard et al. (1999)	Measured at 14 dph
Pacific herring (*Clupea pallasii*)	AW ANSCO	Oiled gravel	Embryo/ Larva	4–7	16	Pericardial edema	↑	LWO = 34.4; MWO = 0.72 EC50 = 3.53 ppb $\sum PAH_{41}$	–	Carls et al. (1999)	LWO = less weathered oil; MWO = more weathered oil

(Continued)

Author's personal copy

Table 1 Summary of morphological effects of crude oil exposure in fish.—cont'd

Species	*Oil type*	*Oil prep*	*Life stage/ age at measurement*	*Temp (°C)*	*Oil exposure duration (Days)*	*Process impacted or endpoint*	*Direction of change*	*Lowest effect concentration (μg/L)*	*No effect concentration (μg/L)*	*References*	*Notes*
Pacific herring (*Clupea pallasii*)	AW ANSCO	Oiled gravel	Embryo/ Larva	4–7	16	Craniofacial malformations	↑	MWO = 0.72 EC50 = 0.33 ppb $\sum PAH_{41}$	_	Carls et al. (1999)	LWO = less weathered oil; MWO = more weathered oil
Pacific herring (*Clupea pallasii*)	AW ANSCO	Oiled gravel	Embryo/ Larva	4–7	16	Spinal abnormalities	↑	LWO = 34.3 EC50 = 33.5; MWO = 0.72 EC50 = 3.6 ppb $\sum PAH_{41}$	_	Carls et al. (1999)	LWO = less weathered oil; MWO = more weathered oil
Pacific herring (*Clupea pallasii*)	AW ANSCO	Oiled gravel	Embryo/ Larva	4–7	16	Finfold abnormalities	↑	MWO = 0.72 EC50 = 0.36 ppb $\sum PAH_{41}$	_	Carls et al. (1999)	LWO = less weathered oil; MWO = more weathered oil
Atlantic Killifish (*Fundulus heteroclitus*)	Benzo[k]fluoranthene (BkF), 3,3′,4,4′,5-pentachlorobiphenyl (PCB-126), or a mixture of BkF and fluoranthene (Fl)	DMSO solutions	Embryo/ Larva	27	5	Cardiac teratogenesis	↑	BkF- 300; PCB-126-1; F1-20	_	Clark et al. (2014)	Cardiac deformities increased from embryos in references sites. Embryos from adults from contaminated sites were highly resistant.
Atlantic Killifish (*Fundulus heteroclitus*)	ANSCO and Mesa Light Crude Oil (MLCO)	Oiled sand	Embryo/ Larva	22.5	11	Spinal deformities; pericardial edema	↑	_	_	Couillard (2002)	50% dilution of both oils caused significant spinal deformities 35% MLCO and 50% ANSCO dilutions caused significant pericardial edema ANSCO- 36.3; MLCO- 35.9 μg oil/g sand
Zebrafish (*Danio rerio*)	Phenanthrene	Dissolved in DMSO	Embryo/ Larva	28	2–3	Edema	↑	1000	100	Cypher et al. (2017)	Phenanthrene exposed only
Zebrafish (*Danio rerio*)	DWH/Source Oil B	WAF	Embryo/ Larva	28.5	<5	Cardiac edema; intracranial hemorrhage	↑	_	_	de Soysa et al. (2012)	

Author's personal copy

Mahi Mahi (*Coryphaena hippurus*)	DWH/Source; AW Source; Slick A	HEWAF/CEWAF	Larva	26	2	Percent edema	↑	HEWAF-Source = 2; AW Source = 2; Slick A = 1.5 CEWAF-AW Source = 6.8 $\sum PAH_{50}$	–	Edmunds et al. (2015)	
Mahi Mahi (*Coryphaena hippurus*)	DWH/Source; AW Source	HEWAF	Larva	26	2	Edema area	↑	HEWAF-Source = 4.6; AW Source = 3 $\sum PAH_{50}$	–	Edmunds et al. (2015)	
Mahi Mahi (*Coryphaena hippurus*)	DWH/Source; AW Source; Slick A	HEWAF	Larva	26	2	Abnormalities in body axis or finfolds	No change	–	HEWAF-Source = 20.3; AW Source = 14.6; Slick A = 5.1 CEWAF-Source = 8.5; AW Source = 10.5; Slick A = 16.4 $\sum PAH_{40}$	Edmunds et al. (2015)	
Mahi Mahi (*Coryphaena hippurus*)	DWH/AW Source	HEWAF	Larva	26	2	Cranial malformations or reduction in eye growth	No change	–	HEWAF-AW Source = 14.6 $\sum PAH_{40}$	Edmunds et al. (2015)	
Mahi Mahi (*Coryphaena hippurus*)	DWH/Source; AW Source; Slick A	HEWAF	Larva	26	2	Incidence of pericardial edema EC_{50}	↑	HEWAF-Source = 7.3; AW Source = 5.7; Slick A = 5.1 CEWAF-Source = 11.5; AW Source = 11.3; Slick A = 13 $\sum PAH_{50}$	–	Esbaugh et al. (2016)	
Pink Salmon (*Oncorhynchus gorbuscha*)	ANSCO	Oiled-gravel effluent	Embryo/ Larva	9	50	Cardiac development	Altered	–	–	Gardner et al. (2019)	Exposed to oil as embryos and raised in clean water Cardiac ventricles showed altered shape, thinner compact myocardium and hypertrophy of the spongy myocardium

(Continued)

Author's personal copy

Table 1 Summary of morphological effects of crude oil exposure in fish.—cont'd

Species	*Oil type*	*Oil prep*	*Life stage/ age at measurement*	*Temp (°C)*	*Oil exposure duration (Days)*	*Process impacted or endpoint*	*Direction of change*	*Lowest effect concentration (μg/L)*	*No effect concentration (μg/L)*	*References*	*Notes*
Mahi Mahi (*Coryphaena hippurus*)	DWH/OFS	CEWAF	Embryo/ Larva	25	2	Pericardial edema	No change	–	–	Greer et al. (2019)	Molecular alterations related to cardiotoxicity in the absence of phenotypic differences in cardiac performance
Cod (*Gadus morhua*)	Troll oil	LEWAF	Embryo/ Larva	6	4	Pericardial edema; craniofacial deformities; jaw deformities	↑	–	–	Hansen et al. (2018)	WAFs biodegraded for varying durations. Larvae measured at 3 and 5 dph
Pacific herring (*Clupea pallasii*)	Stormwater runoff	Diluted with dechlorinated municipal water	Embryo/ Larva	10–12	6	Ventricular ballooning; AV angle; end-systolic ventricle area	↓	–	–	Harding et al. (2020)	Doses- 50%, 25%, 12.5% and 0% runoff
Pacific herring (*Clupea pallasii*)	Stormwater runoff	Diluted with dechlorinated municipal water	Embryo/ Larva	10–12	6	Atrium area; looping defects	↑	–	–	Harding et al. (2020)	Doses- 50%, 25%, 12.5% and 0% runoff
Zebrafish (*Danio rerio*)	ANSCO	Weathered and oiled gravel	Embryo/ Larva	28.5	2	Pericardial edema	↑	60 ppb $\sum PAH_{44}$	–	Hicken et al. (2011)	
Zebrafish (*Danio rerio*)	ANSCO	Weathered and oiled gravel	Embryo/ Larva	28.5	2	Ventricular shape- length to width ratio	↓	24–36 ppb $\sum PAH_{44}$	–	Hicken et al. (2011)	Measured in adults exposed as embryos and raised in clean water
Zebrafish (*Danio rerio*)	DWH/Slick; Source	HEWAF	Embryo/ Larva	28.5	1 or 2	Pericardial edema	↑	1 Day- Source = 170 Slick = 34 2 Days- Source = 390 Slick = 84 $\sum PAC_{40}$	–	Incardona et al. (2013)	
Zebrafish (*Danio rerio*)	DWH/Slick; Source	HEWAF	Embryo/ Larva	28.5	2	Intracranial hemorrhage	↑	–	–	Incardona et al. (2013)	Statistical analysis not applied
Zebrafish (*Danio rerio*)	DWH/Slick; Source	HEWAF	Embryo/ Larva and Juvenile	28.5	3	Finfold defects	↑	Source = 100 ppm	Source = 33 ppm	Incardona et al. (2013)	Measured in ppm and not reported in $\sum PAC$

Author's personal copy

BluefinTuna (*Thunnus thynnus*)	DWH/Source	HEWAF	Embryo/ Larva	25	2–3	Morphological abnormalities	↑	8.5 $\sum PAH_{40}$	–	Incardona et al. (2014)	Abnormalities included finfold defects, finfold blisters, upward curvature of body and reduction in eye growth
BluefinTuna (*Thunnus thynnus*)	DWH/Source	HEWAF	Embryo/ Larva	25	2–3	Edema (EC_{50})	↑	0.8 $\sum PAH_{40}$	Threshold- 0.3 –0.6 $\sum PAH_{40}$	Incardona et al. (2014)	
Yellowfin Tuna (*Thunnus albacares*)	DWH/Slick A	HEWAF	Embryo/ Larva	27	2–3	Morphological abnormalities	↑	3.4 $\sum PAH_{40}$	–	Incardona et al. (2014)	Abnormalities included finfold defects, finfold blisters, upward curvature of body and reduction in eye growth
Yellowfin Tuna (*Thunnus albacares*)	DWH/Slick A	HEWAF	Embryo/ Larva	27	2–3	Edema (EC_{50})	↑	2.3 $\sum PAH_{40}$	Threshold- 0.5 –1.3 $\sum PAH_{40}$	Incardona et al. (2014)	
Amberjack (*Seriola dumerili*)	DWH/Source	HEWAF	Embryo/ Larva	25	2–3	Morphological abnormalities	↑	13.8 $\sum PAH_{40}$	–	Incardona et al. (2014)	Abnormalities included finfold defects, finfold blisters, upward curvature of body and reduction in eye growth
Amberjack (*Seriola dumerili*)	DWH/Source	HEWAF	Embryo/ Larva	25	2–3	Edema (EC_{50})	↑	12.4 $\sum PAH_{40}$	Threshold- 1.0 –6.0 $\sum PAH_{40}$	Incardona et al. (2014)	
Pacific herring (*Clupea pallasii*)	ANSCO	Oiled-gravel effluent	Embryo/ Larva	9	8	Pericardial edema	↑	–	–	Incardona et al. (2015)	Morphological defects were assessed in herring embryos on day of transfer
Pacific herring (*Clupea pallasii*)	ANSCO	Oiled-gravel effluent	Juvenile	9	8	Ventricle aspect ratio	↑	–	–	Incardona et al. (2015)	Assessed in juveniles after transfer to clean water
Pacific herring (*Clupea pallasii*)	ANSCO	Oiled-gravel effluent	Juvenile	9	8	Outflow tract angle	↓	–	–	Incardona et al. (2015)	Assessed in juveniles after transfer to clean water

(Continued)

Author's personal copy

Table 1 Summary of morphological effects of crude oil exposure in fish.—cont'd

Species	*Oil type*	*Oil prep*	*Life stage/ age at measurement*	*Temp (°C)*	*Oil exposure duration (Days)*	*Process impacted or endpoint*	*Direction of change*	*Lowest effect concentration (μg/L)*	*No effect concentration (μg/L)*	*References*	*Notes*
Pink Salmon (*Oncorhynchus gorbuscha*)	ANSCO	Oiled-gravel effluent	Embryo/ Larva	9	50	Pericardial edema; yolk sac edema; hemorrhage	↑	–	–	Incardona et al. (2015)	Morphological defects were assessed in hatched pink salmon alevins on day of transfer
Pink Salmon (*Oncorhynchus gorbuscha*)	ANSCO	Oiled-gravel effluent	Juvenile	9	50	Ventricle aspect ratio	↑	12 μg/g tissue $\sum PAH_{41}$	6 μg/g tissue $\sum PAH_{41}$	Incardona et al. (2015)	Assessed in juveniles after transfer to clean water
Pink Salmon (*Oncorhynchus gorbuscha*)	ANSCO	Oiled-gravel effluent	Juvenile	9	50	Outflow tract	↓	–	9.8	Incardona et al. (2015)	Assessed in juveniles after transfer to clean water
Pacific herring (*Clupea pallasii*)	AW ANSCO	Oiled-gravel effluent	Embryo/ Larva	10	10	Ventricle posterior growth	↓	64 ng/g $\sum PAC_{42}$	10 ng/g $\sum PAC_{42}$	Incardona et al. (2021)	Known as ventricular ballooning IC_{50} of ΣPAC 87 ng/g
Pacific herring (*Clupea pallasii*)	AW ANSCO	Oiled-gravel effluent	Embryo/ Larva	10	10	Abnormal trabeculation	↑	140 ng/g $\sum PAC_{42}$	64 ng/g $\sum PAC_{42}$	Incardona et al. (2021)	Formation of the finger-like projections of interior spongy myocardium
Pacific herring (*Clupea pallasii*)	AW ANSCO	Oiled-gravel effluent	Juvenile	10	10	Hypertrophy of spongy myocardium	↑	64 ng/g $\sum PAC_{42}$	–	Incardona et al. (2021)	At 125 dpf, the only surviving herring belonged to the control and 64 ng/g dose groups
Zebrafish (*Danio rerio*)	IHCO and ANSCO	HEWAF and oiled gravel	Embryo/ Larva	28	2–3	Pericardial edema and intracranial hemorrhage	↑	IHCO- 158; ANSCO- 287 $\sum PAH_{38}$	–	Jung et al. (2013)	High frequency of edema also present in oiled gravel exposures
Zebrafish (*Danio rerio*)	IHCO and ANSCO	HEWAF	Embryo/ Larva	28	2	Poor looping	↑	IHCO- 284; ANSCO- 383 $\sum PAH_{38}$	–	Jung et al. (2013)	
Zebrafish (*Danio rerio*)	IHCO and ANSCO	HEWAF	Embryo/ Larva	28	2	Ventricular diastolic diameter	↓	IHCO- 284; ANSCO- 383 $\sum PAH_{38}$	–	Jung et al. (2013)	

Author's personal copy

Sea Bass (*Lateolabrax maculates*)	IHCO	Fresh (FIHCO) and evaporated (EIHCO) treated gravel	Embryo/ Larva	16	2	Pericardial edema; fin defects; spinal curvature	↑	FIHCO (Initial)-716 & (Final)- 182 EIHCO-(Initial)-651& (Final)- 250 ng/L $\sum PAH_{16}$	_	Jung et al. (2015)	Edema also present after 24 h exposure
Olive Flounder (*Paralichthys olivaceus*)	IHCO	Fresh (FIHCO) and evaporated (EIHCO) treated gravel	Embryo/ Larva	16	2	Pericardial edema; fin defects; spinal curvature	↑	FIHCO (Initial)-716 & (Final)- 182 EIHCO-(Initial)-651& (Final)- 250 ng/L $\sum PAH_{16}$	_	Jung et al. (2015)	Edema also present after 24 h exposure
Red Drum (*Sciaenops ocellatus*)	DWH/OFS	HEWAF	Embryo/ Larva	25	2	Pericardial edema	↑	1.8 $\sum PAH_{50}$	1.4 $\sum PAH_{50}$	Khursigara et al. (2017)	$EC_{50} = 2.4$ (2.1–2.7)
Red Drum (*Sciaenops ocellatus*)	DWH/OFS	HEWAF	Embryo/ Larva	25	2	Craniofacial deformities	↑	2.2 $\sum PAH_{50}$	1.8 $\sum PAH_{50}$	Khursigara et al. (2017)	$EC_{50} = 2.2$ (1.9–2.6)
Polar cod (*Boreogadus saida*)	ANSCO	Artificially weathered by distillation	Larva	2	3	Pericardial edema; craniofacial malformations	↑	0.65–1.1 $\sum PAH_{42}$	_	Laurel et al. (2019)	Embryos transferred to clean SW after exposure
Sea Ruffe (*Sebastiscus marmoratus*)	Benzo[a]pyrene (BaP), pyrene (Py) or phenanthrene (Phe)	DMSO solutions	Embryo/ Larva	18	8	Pericardial edema	↑	BaP- 0.01 Py- 1	Py- 0.1 Phe- 1	Li et al. (2011)	
Sea Ruffe (*Sebastiscus marmoratus*)	Benzo[a]pyrene (BaP), pyrene (Py) or phenanthrene (Phe)	DMSO solutions	Embryo/ Larva	18	8	Abnormal dorsal curvature	↑	BaP- 0.01 Py- 0.1 Phe- 1	BaP- 0.01 Py- 0.01 Phe- 0.1	Li et al. (2011)	
Mahi Mahi (*Coryphaena hippurus*)	DWH/Slick A	HEWAF	Embryo/ Larva	27	2	Pericardial edema	↑	1.2 $\sum PAH_{50}$	_	Mager et al. (2014)	
Zebrafish (*Danio rerio*)	DWH	HEWAF	Embryo/ Larva	28	~3	Pericardial area	No change	_	_	Magnuson et al. (2020)	
Pink Salmon (*Oncorhynchus gorbuscha*)	Exxon Valdez Prudhoe Bay oil	Artificially weathered and applied to gravel	Embryo/ Larva	9	209	Yolk sac area	↑	622 μg oil/g gravel $\sum PAH_{40}$	55.2 μg oil/g gravel $\sum PAH_{40}$	Marty et al. (1997a)	
Pink Salmon (*Oncorhynchus gorbuscha*)	Exxon Valdez Prudhoe Bay oil	Artificially weathered and applied to gravel	Embryo/ Larva	9	209	Ascites	↑	622 μg oil/g gravel $\sum PAH_{40}$	55.2 μg oil/g gravel $\sum PAH_{40}$	Marty et al. (1997a)	
Pacific herring (*Clupea pallasii*)	Exxon Valdez Prudhoe Bay oil	OWD	Embryo/ Larva	_	14–20	Ascites	↑	0.48 mg/L	0.24 mg/L	Marty et al. (1997b)	
Pacific herring (*Clupea pallasii*)	Exxon Valdez Prudhoe Bay oil	Environmental Exposure	Embryo/ Larva	_	_	Ascites and pericardial edema	↑	_	_	Marty et al. (1997b)	

(Continued)

Author's personal copy

Table 1 Summary of morphological effects of crude oil exposure in fish.—cont'd

Species	*Oil type*	*Oil prep*	*Life stage/ age at measurement*	*Temp (°C)*	*Oil exposure duration (Days)*	*Process impacted or endpoint*	*Direction of change*	*Lowest effect concentration (μg/L)*	*No effect concentration (μg/L)*	*References*	*Notes*
Atlantic Herring (*Clupea harengus*)	Medium South American crude oil	CEWAF	Embryo/ Larva	9	1	Blue sac disease	↑	EC/LC50- 8.5 mg/L $\sum PAH_{52}$	–	McIntosh et al. (2010)	Rating system for BSD included yolk sac edemas, spinal curvature, swimming ability, craniofacial malformation, and fin rot Age of embryos negatively correlated with sensitivity to oil
Red Drum (*Sciaenops ocellatus*)	DWH	HEWAF/LEWAF	Embryo/ Larva	28	1.5	Pericardial Area	↑	Slick A HEWAF- IC20- 35; IC50- >31.5 Slick B HEWAF- IC20- 35.3; IC50- 53.7 Slick A LEWAF- IC20- 6.7; IC50- 9.6 Slick B LEWAF- IC20- 16.2; IC50- >14.8 $\sum PAH_{50}$	–	Morris et al. (2018)	
Red Drum (*Sciaenops ocellatus*)	DWH	HEWAF/LEWAF	Embryo/ Larva	28	1.5	AV angle	↑	Slick A HEWAF- IC20- 26.6; IC50- >31.5 Slick B HEWAF- IC20- 28.5; IC50- >51.8 Slick A LEWAF- IC20-8.9; IC50- 18.1 Slick B LEWAF- IC20- 18.5; IC50- >14.8 $\sum PAH_{50}$		Morris et al. (2018)	
Japanese Medaka (*Oryzias latipes*)	Elizabeth River sediment extract	Sediment exposure	Embryo/ Larva	27	13	Pericardial edema	↑	50.45 $\sum PAH_{36}$	–	Mu et al. (2017)	
Fathead Minnow (*Pimephales promelas*)	Snow contaminated by oil sands	Meltwater	Embryo/ Larva	25	12–21	Pericardial edema; craniofacial malformations; spinal curvature; hemorrhages	↑	–	–	Parrott et al. (2018)	
Mahi Mahi (*Coryphaena hippurus*)	DWH/OFS	HEWAF	Larva	26 & 30	1	Pericardial and yolk sac edema	↑	26°- 44.1 $\sum PAH_{50}$ 30°- 14.9 $\sum PAH_{50}$	26°- 18.2 $\sum PAH_{50}$ 30°- NA	Pasparakis et al. (2016)	

Author's personal copy

Mahi Mahi (*Coryphaena hippurus*)	DWH/OFS	HEWAF	Larva	26 & 30	1	Edema area	↑	26°- 12.4 $\sum PAH_{50}$ 30°- 14.9 $\sum PAH_{50}$	26°- 7.4 $\sum PAH_{50}$ 30°- 7.8 $\sum PAH_{50}$	Perrichon et al. (2018)	OFS/HEWAF
Mahi Mahi (*Coryphaena hippurus*)	DWH/OFS	HEWAF	Larva	26 & 30	1	Occurrence of intrapericardial hematomas	↑	26°- 44.1 $\sum PAH_{50}$ 30°- 26.6 $\sum PAH_{50}$	26°- NA 30°- NA	Perrichon et al. (2018)	26°- Control- 6%; Oil Exposed- 49% 30°- Control- 0%; Oil Exposed- 32%
Crimson-spotted Rainbowfish (*Melanotaenia fluviatilis*)	Bass Strait crude oil	CEWAF	Embryo/ Larva	24–25	4	Pericardial edema	↑	0.9 mg/L TPH	0.5 mg/L TPH	Pollino and Holdway (2002)	
Crimson-spotted Rainbowfish (*Melanotaenia fluviatilis*)	Bass Strait crude oil	CEWAF	Embryo/ Larva	24–25	4	Jaw abnormality	↑	1.9 mg/L TPH	0.9 mg/L TPH	Pollino and Holdway (2002)	
Zebrafish (*Danio rerio*)	DWH/Sediment from Barataria Bay	Sediment Exposures	Embryo/ Larva	26	4	Edema; musculoskeletal abnormalities;	↑	61 mg tPAH/kg	22 mg tPAH/kg	Raimondo et al. (2014)	Measured in mg tPAH/kg
Japanese Medaka (*Oryzias latipes*)	Dibenzothiophene (DBT), phenanthrene and benz[a] anthracene and their dimethylated congeners	DMSO solutions	Embryo/ Larva	24	18	Pericardial edema	↑	DBT- 200	DBT- 100	Rhodes et al. (2005)	Unsubstituted PAHs showed trends of increased blue sac disease (BSD) relative to dimethylated PAHs
Zebrafish (*Danio rerio*)	Retene	DMSO solutions	Embryo/ Larva	28.5	1–3	Pericardial edema	↑	12.5 μg/mL	–	Scott et al. (2011)	
Atlantic Haddock (*Melanogrammus aeglefinus*)	Heidrun oil blend	Weathered	Embryo/ Larva	7–8	7	Craniofacial malformations; pericardial edema	↑	0.58 $\sum PAH_{32}$	–	Sørhus et al. (2016)	
Yellowtail Kingfish (*Seriola lalandi*)	North West Shelf oil	HEWAF	Embryo/ Larva	25	1.5	Pericardial edema and spinal curvature	↑	–	–	Sweet et al. (2018)	No UV enhanced effect
Black Bream (*Acanthopagrus butcheri*)	North West Shelf oil	HEWAF	Embryo/ Larva	25	0.5	Pericardial edema	↑	–	–	Sweet et al. (2018)	Effect amplified with 100% UV co-exposure
Mahi Mahi (*Coryphaena hippurus*)	DWH/Slick oil; Source oil	HEWAF	Larva	27	2	Pericardial area	↑	Slick oil-(at 48 h) = 12 $\sum PAH_{50}$	Source oil-(at 48 h) = 4.6 $\sum PAH_{50}$	Xu et al. (2016)	
Mahi Mahi (*Coryphaena hippurus*)	DWH/Slick; Source	HEWAF	Larva (48 hpf)	26–27	2	Pericardial area	↑	Slick = 2.37; Source = 12.68 $\sum PAH_{50}$	Source = 7.11 $\sum PAH_{50}$	Xu et al. (2018)	

(Continued)

Author's personal copy

Table 1 Summary of morphological effects of crude oil exposure in fish.—cont'd

Species	*Oil type*	*Oil prep*	*Life stage/ age at measurement*	*Temp (°C)*	*Oil exposure duration (Days)*	*Process impacted or endpoint*	*Direction of change*	*Lowest effect concentration (μg/L)*	*No effect concentration (μg/L)*	*References*	*Notes*
Red Drum (*Sciaenops ocellatus*)	DWH/Slick	HEWAF	Embryo/ Larva	25	2	Spinal curvature & Pericardial area	↑	4.74 $\sum PAH_{50}$	–	Xu et al. (2017a)	
Zebrafish (*Danio rerio*)	Phenanthrene	DMSO solutions	Embryo/ Larva	28.5	3	Cardiac malformations	↑	0.05 nM	–	Zhang et al. (2013)	Pericardial edema, abnormal heart looping and enlarged ventricles

APD- Action potential duration.
ANSCO- Alaska North Slope crude oil.
AW- Artificially weathered.
CEWAF- Chemically-enhanced-water-accommodated- fractions.
EC_{50}- Concentration of drug that gives half maximal response.
HEWAF- High-energy-water-accommodated- fractions.
IHCO- Iranian heavy crude oil.
LC_{50}- Lethal concentration required to kill 50% of population.
LOAEC- Lowest observed adverse effect concentration.
MASS- Massachusetts source oil.
NOEC- No observed effect concentration.
OFS- Oil from the surface.
OWD- Oil-water dispersion.
PAH- Polycyclic aromatic hydrocarbons.
SOB- Source oil B.
TPH- Total petroleum hydrocarbons.
*Effect concentrations in (μg/L) unless stated otherwise.

Author's personal copy

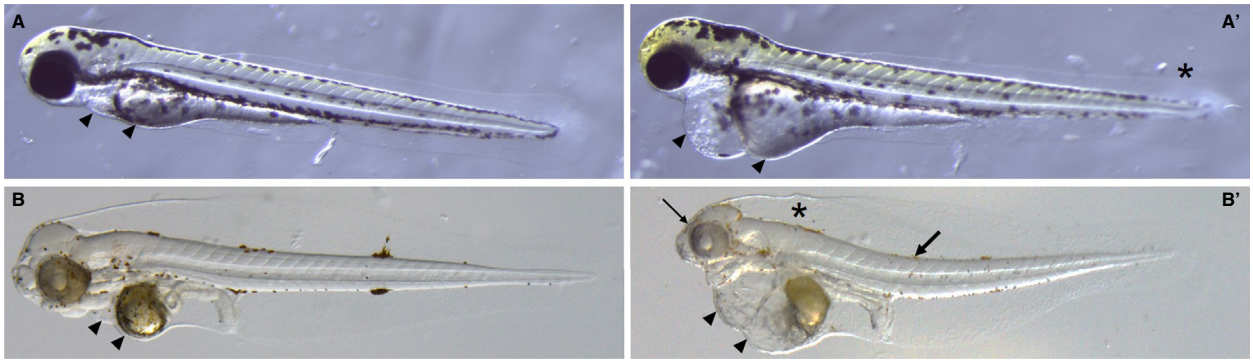

Fig. 3 Light micrograph images of two larval fish species demonstrating the cardiotoxic syndrome of morphological effects following crude oil exposure. Top panels show ~72 h post-fertilization (hpf) zebrafish (*Danio rerio*) exposed to control conditions (A) or slick oil (OFS) from the Deepwater Horizon (DWH) oil spill (467 μg L^{-1} ΣPAH) for 48 h followed by 24 h of recovery in control water (A′) (Bonatesta et al., 2022). Bottom panels show ~72 hpf red drum (*Sciaenops ocellatus*) exposed to control conditions (B) or OFS oil from the DWH oil spill (2.6 μg L^{-1} ΣPAH) for 72 h (B′) (Khursigara et al., 2017). The large difference in exposure concentrations eliciting the cardiotoxic phenotype likely reflect species-specific sensitivities and differences in exposure durations. Pericardial (anterior) and yolk sac (posterior) areas are indicated by arrow heads. Craniofacial malformations and spinal curvature are apparent in the red drum example as indicated by a thin and thick arrow, respectively. Minor alterations to the median finfolds can also be observed in both species as indicated by asterisks.

The fish heart forms initially as a tube-like structure of mesodermal derivation that subsequently undergoes a concomitant increase in length and rightward looping that brings the developing ventricle adjacent to the atrium. These processes are then followed by a ventricular outgrowth (ballooning) and subsequent formation of a spongy myocardium characterized by the growth of ventricular projections known as trabeculae. The muscular trabeculae are thought to increase surface area and flexibility within the ventricle to maximize tissue oxygenation and contractile function, respectively, in the absence of a coronary circulation (which may or may not develop later, depending on the species). For highly athletic or hypoxia tolerant species that rely on a coronary blood supply to supplement the venous oxygen supply route through the heart, a compact myocardium also forms that encases the spongy myocardium during the late larval to juvenile period (Farrell et al., 2009). In zebrafish, where most work in this area has been performed, the timing of these key developmental events has been well established (Brown et al., 2016). Contraction of the still tubular heart is initiated around 24 h post-fertilization (hpf) followed by tubular extension and looping initiated around 28 hpf. By 48 hpf, cardiac looping is complete and a clear division into a two-chambered heart can be observed. Subsequently, at approximately 72 hpf, trabecular ridges become clearly visible and continue to expand as the heart matures. The trabeculae then undergo remodeling (also known as consolidation or compaction), a process that indicates the final stage of trabecular growth and generally leads to the final adult trabecular morphology.

Crude oil exposure to ELS fishes alters the normal patterning of heart development and is typically characterized by failed looping and reduced ventricular cardiomyocyte proliferation (Incardona, 2017). Such alterations in heart morphology have been measured in several ways, including atrioventricular angle and sinus venosus-yolk mass gap (e.g., Edmunds et al., 2015) and areas/volumes of the atrium and ventricle at end diastole and end systole (with volumes conventionally estimated using a prolate spheroid shape) (e.g., Incardona et al., 2021; Perrichon et al., 2017). More recently, measures of cardiac ballooning, cardiac jelly and vessel wall thicknesses and trabecular spacing have been employed (Incardona et al., 2021). Importantly, these alterations in cardiac morphology consistently arise after the heart has started beating, suggesting a functional cardiac impairment rather than an effect on primary cardiac morphogenesis (Incardona et al., 2004; Mager et al., 2017). For example, studies of zebrafish have demonstrated that development of the cardiotoxic syndrome coincides with exposure during the period approximately 12 h after onset of the heart beat (~24 hpf) and during formation of the atrioventricular conduction pathway (Incardona et al., 2004, 2013). Onset of the heartbeat in some large predatory pelagic fishes, such as mahi-mahi (*Coryphaena hippurus*) and others, also begins at ~24 hpf and the cardiac syndrome is clearly present by approximately 48 h of crude oil exposure (~12 h following hatch) (Esbaugh et al., 2016; Incardona et al., 2014; Mager et al., 2014, 2017). These findings therefore support the contention that morphological alterations to the heart likely arise from crude oil-induced impairments in cardiac performance.

The altered shape and reduced contractility of the early heart following crude oil exposure is putatively believed to elicit the downstream morphological sequelae previously described as a result of reduced cardiac function, likely due to a loss of hemodynamic force and shear stress within the vasculature. Indeed, loss-of-function zebrafish mutants, such as *silent heart* (*sih*) that fail to produce a heartbeat, strongly support the role of these hemodynamic factors in the proper development of spinal and craniofacial structures, the pronephros (i.e., primordial kidney), and in the formation of pericardial edema (Incardona et al., 2004). Normal contractility in the early heart is also required for proper formation of the trabeculae (Staudt et al., 2014).

As noted earlier, the most commonly reported injury among the suite of cardiotoxic effects of crude oil exposure is pericardial and yolk sac edema. While identification of the precise mechanism of edema remains somewhat elusive, it is generally thought to arise as a secondary consequence of reduced cardiac output by a failing heart. A relationship between reduced cardiac output and

Author's personal copy

edema formation was supported by proportional changes in the two variables following crude oil exposure to ELS red drum (*Sciaenops ocellatus*) (Khursigara et al., 2017). However, it remains unclear as to whether stroke volume is constrained by the increased hydrostatic pressure from the edema, reducing cardiac output, or if in fact impaired cardiac function initiates the edema. In any event, an interesting and somewhat puzzling observance is that edema formation occurs in response to crude oil exposure regardless of the osmolarity of the surrounding environment. This seems counterintuitive for marine and estuarine fishes that live in hyperosmotic environments as the osmotic gradient favors a loss of water from the animal. Moreover, reduced renal clearance as a result of impaired pronephros formation likely contributes to edema formation to some extent in freshwater species, whereas this role would be expected to be diminished in marine species that rely less on renal fluid clearance for osmoregulation. Incardona and Scholz (2016) have proposed that edema formation in these osmotically divergent environments can be explained by anatomical differences in the membrane compartments of the heart and yolk sac and their vascular elements. In brief, it was proposed that pericardial edema in marine larvae is not the result of whole-body fluid accumulation or reduced fluid clearance, but rather a fluid shift from the subdermal space within the large dorsal finfold to the yolk sac sinus and ultimately the region surrounding the heart. The authors suggested that a gradient of high NaCl in the yolk sac owing to its relatively high surface area is the driving force for this fluid translocation. While intriguing, this potential mechanism clearly warrants further investigation.

Functional effects

Functional analyses of the cardiotoxic effects of crude oil have included relatively simple *in situ* microscopic video assessments of heart rate, contractility and rhythm, and more sophisticated approaches, such as electrophysiological measurements on isolated cardiomyocytes, contractile analyses using isolated hearts or ventricular strips, and measurements of mitochondrial function. With respect to effects on heart rate, contractility, and rhythm, as indicated in **Table 2**, the trend for crude oil-exposed ELS fishes is a decrease in heart rate and contractility and an increase in the prevalence of arrhythmias. However, the significance of a reduced heart rate must be considered in conjunction with stroke volume whenever possible, as it is the product of both of these parameters that determine the more functionally important measure of cardiac output. As one might imagine, measuring stroke volume in extremely small larvae is technically challenging, though recent approaches have been developed to facilitate measurements of this kind as alluded to in the previous section (e.g., Perrichon et al., 2017). In any case, the functional significance of heart rate in the absence of stroke volume (and vice versa) should be regarded with caution. For example, a recent study of crude oil-exposed zebrafish larvae revealed a bradycardia effect, but no change in stroke volume or cardiac output (Magnuson et al., 2020). Consequently, the authors questioned whether the other crude oil effects (in this case related to visual impairment) were dependent on proper cardiac function. Another study examined various parameters of heart function *in situ* by using juvenile cobia (*Rachycentron canadum*) in incremental swimming velocity tests to assess the effect of oil exposure on heart function during exercise (Nelson et al., 2017). It was found that while a general reduction in cardiac output occurred in response to a prior 24 h crude oil exposure at intermediate swimming speeds, this effect was offset by increases in heart rate at higher speeds approaching U_{crit} (i.e., maximum sustained swimming speed). As these examples highlight, reliance on a single contributor to cardiac output could lead to spurious interpretations and conclusions.

Assessments of cardiac arrhythmias, such as prolongation of atrial systole and interbeat variability (e.g., Incardona et al., 2014), as well as heart contractility (e.g., Esbaugh et al., 2016), have also been described in response to ELS crude oil exposure. Perhaps most importantly, these effects likely signify specific molecular cardiac targets for binding by crude oil constituents. Indeed, electrophysiological studies on isolated cardiomyocytes from later life stage fishes have yielded additional insights that largely substantiate the non-AhR receptor-based hypothesis of crude oil induced cardiotoxicity. For example, Brette and colleagues demonstrated that exposure to DWH crude oil water-accommodated fractions (WAFs) at low ΣPAH concentrations prolonged action potential duration and disrupted EC coupling in isolated ventricular myocytes of two tuna species via effects on the delayed rectifier potassium current (I_{Kr}), calcium current (I_{Ca}) and calcium cycling (Brette et al., 2014). A follow-up study investigated the exposure effects of several select individual 2- to 4-ring PAHs on three scombrid species, revealing that only the tricyclic PAH phenanthrene elicited similar electrophysiological responses as seen previously using crude oil WAFs (Brette et al., 2017). These findings provided further support that phenanthrene is likely a key constituent within crude oil driving the cardiotoxic phenotype. However, it should be noted that rather high nominal exposure concentrations (5 μM, or ~0.9 mg L^{-1} for phenanthrene) of the individual PAHs were used in this study, although these were justified by the authors by approaching tissue concentrations measured in oil-exposed embryos from previous studies (Incardona et al., 2009; Jung et al., 2015).

Similar subsequent studies on rainbow trout (*Oncorhynchus mykiss*) (Vehniäinen et al., 2019), brown trout (*Salmo trutta*) (Ainerua et al., 2020), mahi-mahi (Heuer et al., 2019) and navaga cod (*Eleginus nawaga*) (Abramochkin et al., 2021) largely substantiated the prior electrophysiological findings with scombrid fishes. A notable exception is that ion channel disruption led to shortening rather than prolongation of the action potential duration in rainbow trout that was attributed to an increase in the fast Na^+ current (I_{Na}) despite reductions in I_{Ca} and I_{Kr} (Vehniäinen et al., 2019). Additionally, the study by Heuer et al. (2019) confirmed that the observed electrophysiological responses in mahi-mahi exposed to a very low ΣPAH concentration (2.8 μg L^{-1}) translated into reduced heart contractility, supporting the prior *in situ* results of Nelson and colleagues using this same species (Nelson et al., 2016). The latter studies in particular provide important insight that had been inferred but not specifically addressed in prior electrophysiological studies on other species.

Author's personal copy

Table 2 Summary of functional effects of crude oil exposure in fish.

Species	*Oil type*	*Oil prep*	*Life stage/ age at measurement*	*Temp (°C)*	*Oil exposure duration (Days)*	*Process impacted or endpoint*	*Direction of change*	*Lowest effect concentration (μg/L)*	*No effect concentration (μg/L)*	*References*	*Notes*
Navaga Cod (*Eleginus nawaga*)	Phenanthrene	DMSO solutions	Adult	11–13	0	Action potential duration	↑	10 uM	3 uM	Abramochkin et al. (2021)	At both APD 50% and APD 90% Resting membrane potential, AP amplitude and maximal upstroke velocity not affected
Navaga Cod (*Eleginus nawaga*)	Phenanthrene	DMSO solutions	Adult	11–13	0	I_{Kr}	↓	1 uM	–	Abramochkin et al. (2021)	
Navaga Cod (*Eleginus nawaga*)	Phenanthrene	DMSO solutions	Adult	11–13	0	I_{K1} and I_{KACh}	No change	–	30 uM	Abramochkin et al. (2021)	
Navaga Cod (*Eleginus nawaga*)	Phenanthrene	DMSO solutions	Adult	11–13	0	I_{NA}	↓	3 uM	1 uM	Abramochkin et al. (2021)	
Inland Silverside (*Menidia beryllina*)	DWH/Leaking well riser by BP	WAF/CEWAF	Embryo/ Larva	21	3	Heart rate	↓	Oil/9527 = 217.26 $\sum PAH_{47}$	Oil = 24.08; Oil/ 9500 = 44.18 $\sum PAH_{47}$	Adeyemo et al. (2015)	Corexit 9500 & 9527 added to oil preparations
Brown Trout (*Salmo trutta*)	Phenanthrene	DMSO solutions	Adult	10	0	QT interval (time between ventricular depolarization and repolarization) of electrocardiogram	↑	5 uM	–	Ainerua et al. (2020)	Indicative of arrhythmia risk
Brown Trout (*Salmo trutta*)	Phenanthrene	DMSO solutions	Adult	10	0	Cardiac contractility	↓	15 uM	–	Ainerua et al. (2020)	
Brown Trout (*Salmo trutta*)	Phenanthrene	DMSO solutions	Adult	10	0	Action potential duration	Varied	APD 90% = ↑- 10 uM; APD 50% = ↓- 30 uM	–	Ainerua et al. (2020)	
Brown Trout (*Salmo trutta*)	Phenanthrene	DMSO solutions	Adult	10	0	I_{Kr}	↓	10 uM	–	Ainerua et al. (2020)	
Brown Trout (*Salmo trutta*)	Phenanthrene	DMSO solutions	Adult	10	0	I_{CaL}	↓	30 uM	10 uM	Ainerua et al. (2020)	
Rainbow Trout (*Oncorhynchus mykiss*)	Russian Export Blend medium crude oil	Weathered	Juvenile	16	2	Heart rate	↓	4.5 $\sum PAH_{16}$	–	Anttila et al. (2017)	No differences in heart rate at higher temperatures

(Continued)

Author's personal copy

Table 2 Summary of functional effects of crude oil exposure in fish.—cont'd

Species	*Oil type*	*Oil prep*	*Life stage/ age at measurement*	*Temp (°C)*	*Oil exposure duration (Days)*	*Process impacted or endpoint*	*Direction of change*	*Lowest effect concentration (μg/L)*	*No effect concentration (μg/L)*	*References*	*Notes*
European Sea Bass (*Dicentrarchus labrax*)	Arabian light crude oil	Weathered and treated with dispersant	Juvenile	10	2	Heart rate	↓	34.299 ng/g $\sum PAH_{21}$	–	Anttila et al. (2017)	No differences in heart rate at higher temperatures
Siamese Fighting Fish (*Betta splendens*)	DWH/Source Oil B	HEWAF- Dietary exposure	Adult	29	28	Hematocrit	↑	50% HEWAF	–	Bautista et al. (2019)	
Zebrafish (*Danio rerio*)	DWH/Source Oil B	HEWAF- Dietary exposure	Embryo/ Larva	28	21	Heart rate	↓	–	–	Bautista et al. (2020)	Adult zebrafish exposed to oiled diet and heart rate assessed in offspring
Sheepshead Minnow (*Cyprinodon variegatus*)	DWH/Macondo Crude Oil	CEWAF	Embryo/ Larva	26	2	Heart rate	↓	–	–	Bosker et al. (2017)	Full analysis of PAH concentrations not performed
Bluefin Tuna (*Thunnus orientalis*)	DWH/Source; Slick A; Slick B; Weathered	HEWAF	Adult	20	<1	Action potential duration (50%)	↑	Source = 30; Slick A = 4; Slick B = 6 $\sum PAH_{40}$	Source = 15; Weathered = 9 $\sum PAH_{40}$	Brette et al. (2014)	
Bluefin Tuna (*Thunnus orientalis*)	DWH/Source; Slick A; Slick B; Weathered	HEWAF	Adult	20	<1	Resting membrane potential	No change	–	Source = 61; Weathered = 36; Slick A = 14; Slick B = 22 $\sum PAH_{40}$	Brette et al. (2014)	
Bluefin Tuna (*Thunnus orientalis*)	DWH/Slick A; Slick B	HEWAF	Adult	20	<1	K^+ current (I_{Kr})	↓	Slick A = 7; Slick B = 6 $\sum PAH_{40}$	Slick A = 4 $\sum PAH_{40}$	Brette et al. (2014)	
Bluefin Tuna (*Thunnus orientalis*)	DWH/Slick B	HEWAF	Adult	20	<1	Ca^{2+} current (I_{Ca})	↓	Slick B = 6 $\sum PAH_{40}$	–	Brette et al. (2014)	
Yellowfin Tuna (*Thunnus albacares*)	DWH/Source; Slick B	HEWAF	Adult	20	<1	Action potential duration (50%)	↑	Source = 61 $\sum PAH_{40}$	Source = 30; Slick B = 22 $\sum PAH_{40}$	Brette et al. (2014)	
Yellowfin Tuna (*Thunnus albacares*)	DWH/Source; Slick B	HEWAF	Adult	20	<1	Resting membrane potential	No change	–	Source = 61; Slick B = 22 $\sum PAH_{40}$	Brette et al. (2014)	
Yellowfin Tuna (*Thunnus albacares*)	DWH/Slick B	HEWAF	Adult	20	<1	K^+ current (I_{Kr}) & Ca^{2+} current (I_{Ca})	↓	Slick B = 6 $\sum PAH_{40}$	–	Brette et al. (2014)	

Author's personal copy

Bluefin Tuna (*Thunnus orientalis*)	Phenanthrene	Constituted in dimethyl sulfoxide	Adult	20	<1	Ca^{2+} transient amplitude and decay rate	↓	Phenanthrene-5 uM	_	Brette et al. (2017)	Cardiomyocytes exposed to 6 individual PAHs-Napthalene, Fluorene, Carbazole, Dibenzothiophene, Phenanthrene, Pyrene
Bluefin Tuna (*Thunnus orientalis*)	Phenanthrene	Constituted in dimethyl sulfoxide	Adult	20	<1	Resting membrane potential and action potential amplitude	No change	_	Phenanthrene-5 uM	Brette et al. (2017)	Cardiomyocytes exposed to 6 individual PAHs-Napthalene, Fluorene, Carbazole, Dibenzothiophene, Phenanthrene, Pyrene
Yellowfin Tuna (*Thunnus albacares*)	Phenanthrene	Constituted in dimethyl sulfoxide	Adult	20	<1	Ca^{2+} transient amplitude and decay rate	↓	Phenanthrene-5 uM	_	Brette et al. (2017)	Cardiomyocytes exposed to 6 individual PAHs-Napthalene, Fluorene, Carbazole, Dibenzothiophene, Phenanthrene, Pyrene
Pacific Chub Mackerel (*Scomber japonicus*)	Phenanthrene	Constituted in dimethyl sulfoxide	Adult	20	<1	Ca^{2+} transient amplitude and decay rate	↓	5 uM	_	Brette et al. (2017)	Cardiomyocytes exposed to 6 individual PAHs-Napthalene, Fluorene, Carbazole, Dibenzothiophene, Phenanthrene, Pyrene
Common Sole (*Solea solea*)	Number-2 fuel-comparable to oil in tanker ERIKA	_	Adult	15–16	5	Cardiac output; stroke volume; heart rate	↓	_	_	Claireaux and Davoodi (2010)	Decreases in cardiac function depend on test temperatures
Cobia (*Rachycentron canadum*)	DWH/OFS	HEWAF	Young adult	26	1	Cardiac power output	↓	14.1 $\sum PAH_{50}$	NA $\sum PAH_{50}$	Cox et al. (2017)	Explored the protective capabilities of B-adrenergic stimulation
Zebrafish (*Danio rerio*)	Phenanthrene	Dissolved in DMSO	Embryo/Larva	28	2–3	Heart rate; stroke volume; cardiac output; arterial velocity	↓	1000	100	Cypher et al. (2017)	Phenanthrene exposed only
Zebrafish (*Danio rerio*)	DWH/Source Oil B	WAF	Embryo/Larva	28.5	<5	Circulation and vasculogenesis	Altered	_	_	de Soysa et al. (2012)	

(Continued)

Author's personal copy

Table 2 Summary of functional effects of crude oil exposure in fish.—cont'd

Species	*Oil type*	*Oil prep*	*Life stage/ age at measurement*	*Temp (°C)*	*Oil exposure duration (Days)*	*Process impacted or endpoint*	*Direction of change*	*Lowest effect concentration (μg/L)*	*No effect concentration (μg/L)*	*References*	*Notes*
Gulf Killifish (*Fundulus grandis*)	DWH/Sediment from Grand Terre Island	Sediment Exposures	Embryo/ Larva	21	21	Heart rate	↓	–	–	Dubansky et al. (2013)	
Polar cod (*Boreogadus saida*)	Arabian light crude oil	Weathered	Adult	5.4	2	O2 consumption of permeabilized cardiac muscle fibers	↓	40 mg/L ∑PAH	–	Dussauze et al. (2014)	
Mahi Mahi (*Coryphaena hippurus*)	DWH/AW Source	HEWAF/CEWAF	Larva	26	2	Sinus venosus-yolk mass gap	↑	HEWAF-AW Source = 2 CEWAF-AW Source = 2.6 $\sum PAH_{50}$	–	Edmunds et al. (2015)	
Mahi Mahi (*Coryphaena hippurus*)	DWH/Source	HEWAF	Larva	26	2	Atrio-ventricular angle	↑	HEWAF-Source = 16.4 $\sum PAH_{50}$	–	Edmunds et al. (2015)	
Mahi Mahi (*Coryphaena hippurus*)	DWH/Source	HEWAF	Larva	26	2	Fractional shortening	↓	HEWAF-Source = 10.9 $\sum PAH_{50}$	–	Edmunds et al. (2015)	
Mahi Mahi (*Coryphaena hippurus*)	DWH/Source	HEWAF	Larva	26	2	Heart rate	No change	–	HEWAF Source = 11.4 $\sum PAH_{40}$	Edmunds et al. (2015)	
Mahi Mahi (*Coryphaena hippurus*)	DWH/Source; AW Source; Slick A	HEWAF	Larva	26	2	Atrial contractility	↓	HEWAF-Source = 21.6; AW Source = 15.9; Slick A = 4.8 CEWAF-Source = 2.4; AW Source = 5.4; Slick A = 3.5 $\sum PAH_{50}$	HEWAF-Source = 10.3; AW Source = 7.9; Slick A = 1.2 CEWAF-Source = 1.2; AW Source = 2.7; Slick A = 0.3 $\sum PAH_{50}$	Esbaugh et al. (2016)	
Zebrafish (*Danio rerio*)	Benzo-a-pyrene	DMSO solutions aqueous and injected exposures	Adult	28	2	Stroke volume	↓	Aqueous- 162	Aqueous- 16.2; Injected- 1000 μg/kg	Gerger and Weber (2015)	
Zebrafish (*Danio rerio*)	Benzo-a-pyrene	DMSO solutions-aqueous and injected exposures	Adult	28	2	End systolic/diastolic volume	↓	Aqueous- 16.2; Injected- 10 μg/kg	Injected- 0.1 μg/kg	Gerger and Weber (2015)	
Zebrafish (*Danio rerio*)	Benzo-a-pyrene	DMSO solutions-aqueous and injected exposures	Adult	28	2	Ventricular heart rate	↓	Aqueous- 162; Injected- 1000 μg/kg	Aqueous- 16.2; Injected- 10 μg/kg	Gerger and Weber (2015)	

Author's personal copy

Mahi Mahi (*Coryphaena hippurus*)	DWH/OFS	CEWAF	Embryo/ Larva	25	2	Heart rate	No change	_	_	Greer et al. (2019)	Molecular alterations related to cardiotoxicity in the absence of phenotypic differences in cardiac performance
Cod (*Gadus morhua*)	Troll Oil	LEWAF	Embryo/ Larva	6	4	Heart rate	↓	_	_	Hansen et al. (2018)	WAFs biodegraded for varying durations. Larvae measured at 3 and 5 dph
Pacific herring (*Clupea pallasii*)	Stormwater runoff	Diluted with dechlorinated municipal water	Embryo/ Larva	10–12	6	Contractility of ventricle	↑	_	_	Harding et al. (2020)	Doses- 50%, 25%, 12.5% and 0% runoff
Mahi Mahi (*Coryphaena hippurus*)	DWH/OFS	HEWAF	Adult	25–29	0	Sarcomere shortening (contractility)	↓	2.8	_	Heuer et al. (2019)	
Mahi Mahi (*Coryphaena hippurus*)	DWH/OFS	HEWAF	Adult	25–29	0	Action potential duration (APD)	↑	APD 50%- 30.4; APD 20%- 10.6	APD 50%- 10.6; APD 20%- 4	Heuer et al. (2019)	
Mahi Mahi (*Coryphaena hippurus*)	DWH/OFS	HEWAF	Adult	25–29	0	Resting membrane potential; peak amplitude of membrane potential	No change	_	30.4	Heuer et al. (2019)	
Mahi Mahi (*Coryphaena hippurus*)	DWH/OFS	HEWAF	Adult	25–29	0	Peak I_{kr}	↓	9.9	9.3	Heuer et al. (2019)	
Mahi Mahi (*Coryphaena hippurus*)	DWH/OFS	HEWAF	Adult	25–29	0	Peak I_{k1}	No change	_	7.4	Heuer et al. (2019)	
Bluefin Tuna (*Thunnus orientalis*)	DWH/Source	HEWAF	Embryo/ Larva	25	2–3	Heart rate (IC_{50})	↓	7.7 $\sum PAH_{40}$	Threshold- 4.0 –8.5 $\sum PAH_{40}$	Incardona et al. (2014)	
Yellowfin Tuna (*Thunnus albacares*)	DWH/Slick A	HEWAF	Embryo/ Larva	27	2–3	Heart rate (IC_{50})	↓	6.1 $\sum PAH_{40}$	Threshold- 1.0 –2.6 $\sum PAH_{40}$	Incardona et al. (2014)	
Yellowfin Tuna (*Thunnus albacares*)	DWH/Slick A	HEWAF	Embryo/ Larva	27	2–3	Arrhythmia (EC_{50})	↑	2.6 $\sum PAH_{40}$	Threshold- 0.026 –0.13 $\sum PAH_{40}$	Incardona et al. (2014)	
Amberjack *(Seriola dumerili)*	DWH/Source	HEWAF	Embryo/ Larva	25	2–3	Heart rate (IC_{50})	↓	18.2 $\sum PAH_{40}$	Threshold- 2.2 –6.5 $\sum PAH_{40}$	Incardona et al. (2014)	
Amberjack *(Seriola dumerili)*	DWH/Source	HEWAF	Embryo/ Larva	25	2–3	Arrhythmia (EC_{50})	↑	8.6 $\sum PAH_{40}$	Threshold- 0.27 –1.0 $\sum PAH_{40}$	Incardona et al. (2014)	
Amberjack *(Seriola dumerili)*	DWH/Source	HEWAF	Embryo/ Larva	25	2–3	Heartbeat irregularity	↑	13.8 $\sum PAH_{40}$	4.5 $\sum PAH_{40}$	Incardona et al. (2014)	

(Continued)

Author's personal copy

Table 2 Summary of functional effects of crude oil exposure in fish.—cont'd

Species	*Oil type*	*Oil prep*	*Life stage/ age at measurement*	*Temp (°C)*	*Oil exposure duration (Days)*	*Process impacted or endpoint*	*Direction of change*	*Lowest effect concentration (μg/L)*	*No effect concentration (μg/L)*	*References*	*Notes*
Zebrafish (*Danio rerio*)	DWH/Slick; Source	HEWAF	Embryo/ Larva	28.5	1	Atrial Regurgitation	↑	Source = 170 $\sum PAC_{40}$	Slick = 34 $\sum PAC_{40}$	Incardona et al. (2013)	
Zebrafish (*Danio rerio*)	DWH/Slick; Source	HEWAF	Embryo/ Larva and Juvenile	28.5	1	Cardiac contractility	↓	Source = 100 ppm	_	Incardona et al. (2013)	Measured in ppm and not reported in Sum PACs
Zebrafish (*Danio rerio*)	IHCO and ANSCO	HEWAF	Embryo/ Larva	28	2	Ventricular contractility	↓	IHCO- 284; ANSCO- 383 $\sum PAH_{38}$	_	Jung et al. (2013)	
Mahi Mahi (*Coryphaena hippurus*)	DWH/OFS	HEWAF	Juvenile	26	1	Mitochondrial respiration rate	↓	9.6 $\sum PAH_{50}$	_	Kirby et al. (2019)	$OXPHOS_{C1,}$ $OXPHOS_{C1,CII}$ & $OXPHOS_{C1I}$ – Reduced respiration $OXPHOS_{C1V}$- No affect
Mahi Mahi (*Coryphaena hippurus*)	DWH/OFS	HEWAF	Juvenile	26	1	Citrate synthase activity & Activity of key enzymes in mitochondrial complexes I, II, IV and V	No change	_	9.6 $\sum PAH_{50}$	Kirby et al. (2019)	
Mahi Mahi (*Coryphaena hippurus*)	DWH/OFS	HEWAF	Juvenile	26	1	K_{mADP}	↑	9.6 $\sum PAH_{50}$	_	Kirby et al. (2019)	Mitochondrial affinity for ADP decreased by 3-fold
Red Drum (*Sciaenops ocellatus*)	DWH/OFS	HEWAF	Embryo/ Larva	25	2	Heart rate	↓	2.6 $\sum PAH_{50}$	2.2 $\sum PAH_{50}$	Khursigara et al. (2017)	
Red Drum (*Sciaenops ocellatus*)	DWH/OFS	HEWAF	Embryo/ Larva	25	2	Cardiac output & Stroke volume	↓	1.8 $\sum PAH_{50}$	1.4 $\sum PAH_{50}$	Khursigara et al. (2017)	Cardiac output- EC_{50} = 2.2 (2.1–2.3)
Polar cod (*Boreogadus saida*)	ANSCO	Artificially weathered by distillation	Embryo/ Larva	2	3	Bradycardia; abnormal heart rhythms; duration between heartbeats;	↑	_	_	Laurel et al. (2019)	Measured in 27 dpf embryos. Larvae at 42 dpf still displayed bradycardia but no rhythm irregularities
Mahi Mahi (*Coryphaena hippurus*)	DWH/Slick A	HEWAF	Embryo/ Larva	27	2	Heart rate	No change	_	1.2 $\sum PAH_{50}$	Mager et al. (2014)	
Zebrafish (*Danio rerio*)	DWH crude oil	HEWAF	Embryo/ Larva	28	~3	Heart rate	↓	64.2 $\sum PAH_{50}$	38.5 $\sum PAH_{50}$	Magnuson et al. (2020)	

Author's personal copy

Zebrafish (*Danio rerio*)	DWH crude oil	HEWAF	Embryo/ Larva	28	~3	Stroke volume; cardiac output	No change	–	–	Magnuson et al. (2020)
Inland Silverside (*Menidia beryllina*)	ANSCO	Weathered and microbially degraded	Embryo/ Larva	25	7–10	Cardiac contractions	↓	–	–	Middaugh et al. (2002)
Red Drum (*Sciaenops ocellatus*)	DWH/Slick A; Slick B	HEWAF/LEWAF	Embryo/ Larva	28	1.5	Ventricular contractility	↓	Slick A HEWAF- IC20- 8; IC50- 28.1 Slick B HEWAF- IC20- 5.6; IC50- 19.7 Slick A LEWAF- IC20- 2.8; IC50- 7.3 Slick B LEWAF- IC20- 3.7; IC50- 9.7 $\sum PAH_{50}$	–	Morris et al. (2018)
Red Drum (*Sciaenops ocellatus*)	DWH/Slick A; Slick B	HEWAF/LEWAF	Embryo/ Larva	28	1.5	Atrial contractility	↓	Slick A HEWAF- IC20- 35.5; IC50- >31.5 Slick B HEWAF- IC20- 22.9; IC50- >51.8 Slick A LEWAF- IC20- 6.4; IC50- 20.2 Slick B LEWAF- IC20- 7.8; IC50- >14.8 $\sum PAH_{50}$	–	Morris et al. (2018)
Red Drum (*Sciaenops ocellatus*)	DWH/Slick A; Slick B	HEWAF	Embryo/ Larva	28	1.5	Heart rate	↓	Slick A HEWAF- 31.5 Slick B HEWAF- 51.8 $\sum PAH_{50}$	Slick A HEWAF- 5.9 Slick B HEWAF- 21.1 $\sum PAH_{50}$	Morris et al. (2018)
Mahi Mahi (*Coryphaena hippurus*)	DWH/OFS	HEWAF	Young adult	26	1	Stroke volume, Stroke work, Cardiac output & Heart contractility index	↓	9.6 $\sum PAH_{50}$	–	Nelson et al. (2016)

(Continued)

Author's personal copy

Table 2 Summary of functional effects of crude oil exposure in fish.—cont'd

Species	*Oil type*	*Oil prep*	*Life stage/ age at measurement*	*Temp (°C)*	*Oil exposure duration (Days)*	*Process impacted or endpoint*	*Direction of change*	*Lowest effect concentration (μg/L)*	*No effect concentration (μg/L)*	*References*	*Notes*
Mahi Mahi (*Coryphaena hippurus*)	DWH/OFS	HEWAF	Young adult	26	1	Heart rate & Blood pressure parameters	No change	–	9.6 $\sum PAH_{50}$	Nelson et al. (2016)	Blood pressure parameters- Mean intraventricular pressure; peak developed pressure; end diastolic pressure; end systolic pressure
Cobia (*Rachycentron canadum*)	DWH/Slick	HEWAF	Young adult	26	1	Heart rate	↑	10.52 $\sum PAH_{50}$	5.24 $\sum PAH_{50}$	Nelson et al. (2017)	Parameters measured at different swimming speeds
Cobia (*Rachycentron canadum*)	DWH/Slick	HEWAF	Young adult	26	1	Stroke volume & Cardiac output	↓	10.52 $\sum PAH_{50}$	5.24 $\sum PAH_{50}$	Nelson et al. (2017)	
Mahi Mahi (*Coryphaena hippurus*)	DWH/OFS	HEWAF	Larva	26 & 30	1	Heart rate	↓	26°- 6 $\sum PAH_{50}$ 30°- 14.9 $\sum PAH_{50}$	26°- NA 30°- NA	Pasparakis et al. (2016)	
Mahi Mahi (*Coryphaena hippurus*)	DWH/OFS	HEWAF	Larva	26 & 30	1	Sinus venosus-yolk mass gap	↑	26°- 7.4 $\sum PAH_{50}$ 30°- 26.6 $\sum PAH_{50}$	26°- 3 $\sum PAH_{50}$ 30°- NA	Perrichon et al. (2018)	
Mahi Mahi (*Coryphaena hippurus*)	DWH/OFS	HEWAF	Larva	26 & 30	1	Heart rate	↓	26°- 31.2 $\sum PAH_{50}$ 30°- 14.9 $\sum PAH_{50}$	26°- 12.4 $\sum PAH_{50}$ 30°- 7.8 $\sum PAH_{50}$	Perrichon et al. (2018)	
Mahi Mahi (*Coryphaena hippurus*)	DWH/OFS	HEWAF	Larva	26 & 30	1	Stroke volume	↓	26°- 31.2 $\sum PAH_{50}$ 30°- 26.6 $\sum PAH_{50}$	26°- 12.4 $\sum PAH_{50}$ 30°- 14.9 $\sum PAH_{50}$	Perrichon et al. (2018)	
Mahi Mahi (*Coryphaena hippurus*)	DWH/OFS	HEWAF	Larva	26 & 30	1	Cardiac output	↓	26°- 3 $\sum PAH_{50}$ 30°- 14.9 $\sum PAH_{50}$	26°- NA 30°- 7.8 $\sum PAH_{50}$	Perrichon et al. (2018)	
Zebrafish (*Danio rerio*)	DWH/Source	WAF	Embryo/ Larva	27.5	7	Heart rate	↑	–	–	Philibert et al. (2019)	
Sheepshead Minnow (*Cyprinodon variegatus*)	DWH/Source	WAF	Embryo/ Larva	25.5	10	Heart rate	↓	–	–	Philibert et al. (2019)	
Zebrafish (*Danio rerio*)	Retene	DMSO solutions	Embryo/ Larva	28.5	1–3	Circulation; diastolic filling	↓	12.5 μg/mL	–	Scott et al. (2011)	

Author's personal copy

Atlantic Haddock (*Melanogrammus aeglefinus*)	Heidrun oil blend	Weathered	Embryo/ Larva	7–8	7	Heart rate	↓	6.7 $\sum PAH_{32}$	0.58 $\sum PAH_{32}$	Sørhus et al. (2016)	
Atlantic Haddock (*Melanogrammus aeglefinus*)	Heidrun oil blend	Weathered	Embryo/ Larva	7–8	7	Silent ventricles	↑	0.58 $\sum PAH_{32}$	–	Sørhus et al. (2016)	
Atlantic Haddock (*Melanogrammus aeglefinus*)	Heidrun oil blend	Weathered	Embryo/ Larva	7–8	7	Ventricular and atrial contractility	↓	0.58 $\sum PAH_{32}$	–	Sørhus et al. (2016)	
Mahi Mahi (*Coryphaena hippurus*)	DWH/OFS	HEWAF	Larva	27	1	Heart rate	↓	Late UV co-exposure- = 4 $\sum PAH_{50}$	Late UV co-exposure- = 1 $\sum PAH_{50}$	Sweet et al. (2017)	Bradycardia not observed in oil exposed larvae without UV (NOEC-35)
Yellowtail Kingfish (*Seriola lalandi*)	North West Shelf oil	HEWAF	Embryo/ Larva	25	1.5	Heart rate	↓	–	–	Sweet et al. (2018)	No difference in 10 or 100% UV groups
Yellowtail Kingfish (*Seriola lalandi*)	North West Shelf oil	HEWAF	Embryo/ Larva	25	1.5	Arrhythmia	↑	–	–	Sweet et al. (2018)	Significantly higher in fish co-exposed to 100% UV than in 10% UV
Rainbow Trout (*Oncorhynchus mykiss*)	Phenanthrene and retene	DMSO solutions	Adult	14	0	Action potential (APD 50%)	↓	Retene- 1 uM	Retene- 0.1 uM	Vehniäinen et al. (2019)	
Rainbow Trout (*Oncorhynchus mykiss*)	Phenanthrene and retene	DMSO solutions	Adult	14	0	I_{Na}	↑	Phenanthrene- 10 uM; Retene- 1 uM	–	Vehniäinen et al. (2019)	
Rainbow Trout (*Oncorhynchus mykiss*)	Phenanthrene and retene	DMSO solutions	Adult	14	0	I_{CaL}	↓	Phenanthrene- 30 uM; Retene- 1 uM	Phenanthrene- 10 uM	Vehniäinen et al. (2019)	
Rainbow Trout (*Oncorhynchus mykiss*)	Phenanthrene and retene	DMSO solutions	Adult	14	0	I_{Kr}	↓	Phenanthrene- 10 uM; Retene- 0.1 uM	–	Vehniäinen et al. (2019)	
Rainbow Trout (*Oncorhynchus mykiss*)	Phenanthrene and retene	DMSO solutions	Adult	14	0	I_{K1}	No change	–	–	Vehniäinen et al. (2019)	
Mahi Mahi (*Coryphaena hippurus*)	DWH/Slick oil; Source oil	HEWAF	Embryo/ Larva	27	1,2 and 4	Heart rate	↓	Slick oil-(at 24 and 96 h) = 12 $\sum PAH_{50}$	Source oil-(at 24, 48 and 96 h) = 4.6 $\sum PAH_{50}$	Xu et al. (2016)	Effect of slick oil on HR most pronounced at 96 h

(Continued)

Author's personal copy

Table 2 Summary of functional effects of crude oil exposure in fish.—cont'd

Species	*Oil type*	*Oil prep*	*Life stage/ age at measurement*	*Temp (°C)*	*Oil exposure duration (Days)*	*Process impacted or endpoint*	*Direction of change*	*Lowest effect concentration (μg/L)*	*No effect concentration (μg/L)*	*References*	*Notes*
Mahi Mahi (*Coryphaena hippurus*)	DWH/Slick; Source	HEWAF	Larva (48 hpf)	26–27	2	Heart rate	↓	Slick = 2.37; Source = 12.68 $\sum PAH_{50}$	Source = 31.47 $\sum PAH_{50}$	Xu et al. (2018)	
Zebrafish (*Danio rerio*)	Phenanthrene	DMSO solutions	Embryo/ Larva	28.5	3	Heart rate	↑	0.5 nmol/L	0.05 nmol/L	Zhang et al. (2013)	
Zebrafish (*Danio rerio*)	Phenanthrene	DMSO solutions	Embryo/ Larva	28.5	3	Stroke volume	↓	5 nmol/L	0.5 nmol/L	Zhang et al. (2013)	
Zebrafish (*Danio rerio*)	Phenanthrene	DMSO solutions	Embryo/ Larva	28.5	3	Cardiac output	↓	5 nmol/L	0.5 nmol/L	Zhang et al. (2013)	

APD- Action potential duration.
ANSCO- Alaska North Slope crude oil.
AW- Artificially weathered.
CEWAF- Chemically-enhanced-water-accommodated- fractions.
EC_{50}- Concentration of drug that gives half maximal response.
HEWAF- High-energy-water-accommodated- fractions.
IHCO- Iranian heavy crude oil.
LC_{50}- Lethal concentration required to kill 50% of population.
LOAEC- Lowest observed adverse effect concentration.
MASS- Massachusetts source oil.
NOEC- No observed effect concentration.
OFS- Oil from the surface.
OWD- Oil-water dispersion.
PAH- Polycyclic aromatic hydrocarbons.
SOB- Source oil B.
TPH- Total petroleum hydrocarbons.
*Effect concentrations in (μg/L) unless stated otherwise.

Author's personal copy

Physiological stress, including exercise, elicits the release of intrinsic catecholamine stores, such as adrenaline, that contribute to increased cardiac performance via adrenergic stimulation. Thus, the potential exists for compensation of crude oil induced effects on heart function during bouts of stress by increasing the release of these stores to the bloodstream. Several studies have examined such a role of adrenergic stimulation of heart function in crude oil exposed fishes, namely common sole (*Solea solea*) (Claireaux et al., 2004), grey mullet (*Liza aurata*) (Milinkovitch et al., 2013) and cobia (Cox et al., 2017), using isolated heart strips or *in situ* heart preparations. A consistent finding among these studies is that a positive inotropic (force) effect of adrenergic stimulation on heart function is largely lost in fish exposed to elevated crude oil exposures. These studies used adrenergic stimulants spanning a range of physiologically relevant concentrations of 10^{-9} to 10^{-6} M; however, in the study on cobia, a 10^{-5} M concentration was also used that was sufficient to return heart function of oil exposed fish back to control levels. The authors acknowledged that this concentration was physiologically unlikely to occur within blood, but might be similar to that found within adrenergic nerve synapses (Cox et al., 2017). In any case, the evidence to date suggests that adrenergic stimulation is unlikely to overcome the impacts of crude oil exposure on heart function during conditions of stress.

Finally, several studies have investigated the potential role of impaired mitochondrial function in mediating toxicity within cardiomyocytes of crude oil exposed fishes, such as polar cod (*Boreogadus saida*) (Dussauze et al., 2014), red drum (Johansen and Esbaugh, 2019) and mahi-mahi (Kirby et al., 2019). The heart is a highly aerobic tissue and thus its performance is largely mediated by mitochondrial oxygen consumption and ATP production. Assessments of mitochondrial function thus often rely on measurements of ATP turnover and proton leak across the inner mitochondrial membrane which influences the proton circuit driving ATP production. While some inhibiting effects on electron transport chain complexes have been observed, the general conclusion that can be gleaned from the aforementioned studies is that mitochondrial dysfunction seems unlikely to contribute significantly to the cardiotoxic phenotype.

Molecular effects

The advent of high-throughput RNA sequencing techniques has greatly facilitated analyses of the transcriptional responses of fishes exposed to crude oil and shed new light on the underlying molecular mechanisms of toxicity. Cross-study comparisons are often hampered by differences in target species, developmental stage at initiation, duration of exposure, time points analyzed, and oil types/preparations. Nevertheless, while the transcriptional expression of specific genes may vary across different species or exposure scenarios, the prevalence of others in spite of these differences likely signifies conserved molecular responses. Among the more consistent transcripts identified across studies include members of the *nkx*, *kcn* and *bmp* gene families, as well as myosin heavy (*myh*) and light (*myl*) chain transcripts and others integral to intracellular calcium cycling, including *serca* and *ryr*. Members of the *nkx* gene family are homeobox transcription factors that regulate organ development (Stanfel et al., 2005). Of these, *nkx2.3*, *nkx2.5* and *nkx3.3* have been identified as overexpressed from transcriptional analyses of various crude oil exposed fishes (Incardona et al., 2021; Jung et al., 2017; Philibert et al., 2019; Sørhus et al., 2017). A recent study examined the roles of these transcripts in early zebrafish development. The authors found overlapping functionalities involved in cardiac morphogenesis, thus supporting the overexpression of these transcripts as likely contributing to the crude oil cardiotoxic phenotype (Gardner et al., 2019). Notably, *notch1*, a signaling receptor involved in normal heart development and abnormal hypertrophic responses, was downregulated in the same study. Members of the *kcn* gene family, particularly *kcnh2* (potassium voltage-gated channel subfamily H member 2 (ERG)), have been consistently found to be downregulated following crude oil exposure in ELS fishes (Sørhus et al., 2016, 2017; Xu et al., 2017b). Together with the observed decreased mRNA expression of *serca* (Sørhus et al., 2016, 2017; Xu et al., 2017b) and *ryr* family members (Xu et al., 2016) involved in intracellular calcium cycling, these findings further support the AhR dependent mechanism of crude oil induced cardiotoxicity, as previously described. Bone morphometric protein (*bmp*) family members, specifically *bmp4* and *bmp10*, have been shown to be upregulated (Jung et al., 2017; Sørhus et al., 2017; Xu et al., 2017b), implicating likely roles in the development of heart defects, including cardiac hypertrophy and fibrosis (Sun et al., 2013). Finally, downregulation of a range of genes encoding *myh* and *myl* family members have also been reported (Incardona et al., 2021; Xu et al., 2017b), indicating likely molecular targets of crude oil exposure that directly impact heart contractility.

Intriguing results from two recent complementary studies of ELS mahi-mahi have identified potential roles of altered microRNA (miRNA) expression and their target mRNA interactions in crude oil cardiotoxicity (Diamante et al., 2017; Xu et al., 2018). Among the most differentially expressed miRNAs found with crude oil exposure were five that were upregulated (miR-15b, miR-23b, miR-34b, miR-133, and miR-181b) and one that was downregulated (miR-203a). Analyses of mRNA associations placed the roles of these miRNAs largely within categories known to alter heart development and function, including AhR and cardiac β-adrenergic signaling, in addition to vision (Xu et al., 2018). For example, the miR-15b transcript, members of which have been shown to aid in normal heart development (Porrello et al., 2013), was found to regulate the largest number of differentially expressed mRNAs (Diamante et al., 2017). The miRNA with perhaps the most direct link to a gene transcript previously implicated in the cardiotoxic phenotype was miR-133. Specifically, network analysis correlated miR-133 with expression of *kcnh2*, potentially implicating a role for this miRNA in the disruption of potassium flux during EC coupling by altering expression of this potassium channel (Diamante et al., 2017).

Finally, while transcriptomics studies such as these have provided new evidence in support of the molecular mechanisms of crude oil induced cardiotoxicity, they have also illuminated new areas of research for crude oil induced effects in ELS fishes that may or may not be independent of cardiac impairment. Such effects include alterations to cholesterol biosynthesis, vision and

Author's personal copy

neurological effects, and impairments to the developing liver and kidney (Sørhus et al., 2017; Xu et al., 2016, 2017a,b). Although some of these effects are very likely the downstream result of impaired circulation arising from reduced cardiac function (e.g., liver and kidney development), others such as cholesterol biosynthesis and vision are less tightly linked to cardiovascular effects at this time; however, future studies may ultimately provide these links.

Cardiotoxicity implications: Swimming performance and hypoxia and thermal tolerance

Considering the role of the cardiovascular system in convective oxygen transport, any impairment to cardiac function, such as that arising from crude oil exposure, has the potential to reduce oxygen delivery to the tissues, thereby limiting aerobic performance. Naturally, this will first become evident under conditions of increased oxygen demand, such as during exercise or elevated temperature, or under conditions of low environmental oxygen (i.e., hypoxia). However, given that embryo-larval fish are thought to achieve sufficient uptake of oxygen by simple diffusion across the skin (Burggren et al., 2017), cardiac defects are unlikely to play a significant role related to oxygen acquisition or delivery during ELSs. Hence, the following sections will focus largely on juvenile and adult fishes where oxygen demand is entirely dependent on the cardiovascular system. Still, crude oil exposures during the ELSs may impose subtle alterations to heart development/function that manifest as chronic/latent cardiac effects at these later life stages.

Clearly, acute crude oil exposure can lead to reductions in aerobic swimming performance as determined by measurements of maximum sustained swimming velocity (U_{crit}) (e.g., Johansen and Esbaugh, 2017; Mager et al., 2014; Nelson et al., 2017), although no effect has also been observed (e.g., Milinkovitch et al., 2012). Interestingly, however, reductions in U_{crit} do not always correspond with decreases in aerobic scope (Johansen and Esbaugh, 2017; Mager et al., 2014) suggesting that, at least in some cases, swimming performance is not limited by crude oil induced constraints on oxygen delivery and thus are likely independent of cardiac effects. Transient exposures during the ELSs can nevertheless impart long-lasting detriment to cardiac development and swimming performance, as indicated by grow-out studies (Hicken et al., 2011; Mager et al., 2014). Moreover, chronic crude oil exposure does not appear to lead to acclimation, given that reduced U_{crit} persisted out to at least 8 weeks of continuous exposure to juvenile Pacific herring (*Clupea pallasi*) (Kennedy and Farrell, 2006). Furthermore, recovery in control water for at least 4–6 weeks following an acute 24–48 h crude oil exposure did not alleviate impairments to swimming performance in red drum or European sea bass (*Dicentrarchus labrax*) (Johansen and Esbaugh, 2017; Mauduit et al., 2016), although 10 months was sufficient for full recovery by *D. labrax* (Mauduit et al., 2016).

Although there is currently debate regarding the role of the cardiovascular system as the main determinant of thermal tolerance, as defined by the critical thermal maximum (CT_{max}) (Jutfelt et al., 2018), a number of studies have examined the role of crude oil induced cardiac impairments in this context, as well as in regard to hypoxia tolerance (see Khursigara et al., 2019 for review). In terms of thermal tolerance, the evidence to date is mixed as both improvement (Anttila et al., 2017) and reduction (Claireaux and Davoodi, 2010) as well as no effect (Claireaux et al., 2013; Mauduit et al., 2016, 2019) have been observed following crude oil exposure. Effects on hypoxia tolerance appear more consistent, however, with evidence supporting a decrease in this metric with crude oil exposure in several fish species (Ackerly and Esbaugh, 2020; Mauduit et al., 2016), though other studies have reported no effect on hypoxia tolerance (e.g., Mauduit et al., 2019; Pan et al., 2018). A study of the interactive effects of temperature or hypoxia with crude oil exposure on the swimming performance of juvenile mahi-mahi revealed that either hypoxia alone or hypoxia combined with crude oil exposure reduced U_{crit}, whereas elevated temperature did not; however, these effects were not additive as they elicited similar decreases in U_{crit} (~20%), suggesting they were due to hypoxia alone (Mager et al., 2018). Undoubtedly, there remains much to be learned regarding crude oil induced cardiac impairments and their functional significance in both thermal and hypoxia tolerance.

Conclusions

Crude oil exposure to ELS fishes elicits a characteristic syndrome of cardiotoxic effects, the most prominent and widely-reported of which is pericardial and yolk sac edema. Although the underlying mechanisms of cardiotoxicity remain a subject of debate, recent transcriptional and functional assays have identified intriguing molecular targets with potential roles in both the AhR dependent and independent pathways. The most promising of these include targets directly involved in calcium and potassium fluxes related to cardiomyocyte EC coupling such as SERCA2, RyR2 and ERG. While electrophysiological/pharmacological studies provide strong evidence indicative of an AhR independent mechanism of toxicity based on tricyclic PAHs targeting one or more of these potential receptors, a specific molecular initiating event for any of these has yet to be fully characterized. Nevertheless, alteration of these genes and others related to cardiomyocyte development/function clearly support the AhR dependent mechanism of toxicity. Studies of adrenergic stimulation and mitochondrial function indicate they likely do not contribute significantly to rescuing or explaining crude oil impairments to cardiac function, respectively. While some insightful hypotheses have been proposed to explain the development of pericardial edema in crude oil exposed fishes despite the surrounding osmotic environment, careful follow-up studies are needed to confirm or refute these. Finally, it seems clear that acute crude oil exposures (e.g., 24–48 h), either during the ELS or later life stages, can result in persistent impairments to swimming performance. These are typically, but not always, associated with a reduced aerobic scope, implicating a possible consequence of impaired cardiac function. Other physiological assessments

Author's personal copy

potentially related to cardiac function following crude oil exposure have included hypoxia and thermal tolerance. While crude oil exposure tends to decrease hypoxia tolerance, results from thermal tolerance studies have been less conclusive.

Acknowledgments

The authors would like to thank Fabrizio Bonatesta and Andrew Esbaugh for providing photographs of fish larvae and Terence Gaffney for assistance in figure graphic design.

See Also: Energetics of fish swimming; Excitation-contraction coupling in fish cardiomyocytes; The effects of abiotic factors on olfaction in fishes.

References

Abramochkin, D.V., Kompella, S.N., Shiels, H.A., 2021. Phenanthrene alters the electrical activity of atrial and ventricular myocytes of a polar fish, the Navaga cod. Aquat. Toxicol. 235, 105823. https://doi.org/10.1016/j.aquatox.2021.105823.

Ackerly, K.L., Esbaugh, A.J., 2020. The additive effects of oil exposure and hypoxia on aerobic performance in red drum (*Sciaenops ocellatus*). Sci. Total Environ. 737 (1), 140174. https://doi.org/10.1016/j.scitotenv.2020.140174.

Adeyemo, O.K., Kroll, K.J., Denslow, N.D., 2015. Developmental abnormalities and differential expression of genes induced in oil and dispersant exposed *Menidia beryllina* embryos. Aquat. Toxicol. 168, 60–71. https://doi.org/10.1016/j.aquatox.2015.09.012.

Ainerua, M.O., Tinwell, J., Kompella, S.N., Sørhus, E., White, K.N., van Dongen, B.E., Shiels, H.A., 2020. Understanding the cardiac toxicity of the anthropogenic pollutant phenanthrene on the freshwater indicator species, the brown trout (*Salmo trutta*): from whole heart to cardiomyocytes. Chemosphere 239, 124608. https://doi.org/10.1016/j.chemosphere.2019.124608.

Anttila, K., Mauduit, F., Le Floch, S., Claireaux, G., Nikinmaa, M., 2017. Influence of crude oil exposure on cardiac function and thermal tolerance of juvenile rainbow trout and European sea bass. Environ. Sci. Pollut. Res. Int. 24, 19624–19634. https://doi.org/10.1007/s11356-017-9609-x.

Aranguren-Abadía, L., Yadetie, F., Donald, C.E., Sørhus, E., Myklatun, L.E., Zhang, X., Lie, K.K., Perrichon, P., Nakken, C.L., Durif, C., Shema, S., Browman, H.I., Skiftesvik, A.B., Goksøyr, A., Meier, S., Karlsen, O.A., 2022. Photo-enhanced toxicity of crude oil on early developmental stages of Atlantic cod (*Gadus morhua*). Sci. Total Environ. 807. https://doi.org/10.1016/j.scitotenv.2021.150697.

Barjhoux, I., Cachot, J., Gonzalez, P., Budzinski, H., Le Menach, K., Landi, L., Morin, B., Baudrimont, M., 2014. Transcriptional responses and embryotoxic effects induced by pyrene and methylpyrene in Japanese medaka (*Oryzias latipes*) early life stages exposed to spiked sediments. Environ. Sci. Pollut. Res. Int. 21, 13850–13866. https://doi.org/10.1007/s11356-014-2895-7.

Barron, M.G., Heintz, R., Rice, S.D., 2004. Relative potency of PAHs and heterocycles as aryl hydrocarbon receptor agonists in fish. Mar. Environ. Res. 58, 95–100. https://doi.org/10.1016/j.marenvres.2004.03.001.

Barron, M.G., Vivian, D.N., Heintz, R.A., Yim, U.H., 2020. Long-term ecological impacts from oil spills: comparison of Exxon Valdez, Hebei Spirit, and deepwater horizon. Environ. Sci. Technol. 54, 6456–6467. https://doi.org/10.1021/acs.est.9b05020.

Bautista, N.M., Crespel, A., Crossley, J., Padilla, P., Burggren, W., 2020. Parental transgenerational epigenetic inheritance related to dietary crude oil exposure in *Danio rerio*. J. Exp. Biol. 223 (16), jeb222224. https://doi.org/10.1242/jeb.222224.

Bautista, N.M., Pothini, T., Meng, K., Burggren, W.W., 2019. Behavioral consequences of dietary exposure to crude oil extracts in the Siamese fighting fish (*Betta splendens*). Aquat. Toxicol. 207, 34–42. https://doi.org/10.1016/j.aquatox.2018.11.025.

Billiard, S.M., Querbach, K., Hodson, P.V., 1999. Toxicity of retene to early life stages of two freshwater fish species. Environ. Toxicol. Chem. 18, 2070–2077. https://doi.org/10.1002/etc.5620180927.

Bonatesta, F., Emadi, C., Price, E.R., Wang, Y., Greer, J.B., Xu, E.G., Schlenk, D., Grosell, M., Mager, E.M., 2022. The developing zebrafish kidney is impaired by Deepwater Horizon crude oil early-life stage exposure: a molecular to whole-organism perspective. Sci. Total Environ. 808, 151988. https://doi.org/10.1016/j.scitotenv.2021.151988.

Bosker, T., van Balen, L., Walsh, B., Sepúlveda, M.S., DeGuise, S., Perkins, C., Griffitt, R.J., 2017. The combined effect of Macondo oil and corexit on sheepshead minnow (*Cyprinodon variegatus*) during early development. J. Toxicol. Environ. Health A 80, 477–484. https://doi.org/10.1080/15287394.2017.1340208.

Brette, F., Machado, B., Cros, C., Incardona, J.P., Scholz, N.L., Block, B.A., 2014. Crude oil impairs cardiac excitation-contraction coupling in fish. Science 343, 772–776. https://doi.org/10.1126/science.1242747.

Brette, F., Shiels, H.A., Galli, G.L.J., Cros, C., Incardona, J.P., Scholz, N.L., Block, B.A., 2017. A novel cardiotoxic mechanism for a pervasive global pollutant. Sci. Rep. 7, 41476. https://doi.org/10.1038/srep41476.

Brown, D.R., Samsa, L.A., Qian, L., Liu, J., 2016. Advances in the study of heart development and disease using zebrafish. J. Cardiovasc. Dev. Dis. 3, 13. https://doi.org/10.3390/jcdd3020013.

Burggren, W.W., Dubansky, B., Bautista, N.M., 2017. Cardiovascular development in embryonic and larval fishes. Fish Physiol. 36 (Part B), 107–184. Elsevier.

Carls, M.G., Rice, S.D., Hose, J.E., 1999. Sensitivity of fish embryos to weathered crude oil: Part I. Low-level exposure during incubation causes malformations, genetic damage, and mortality in larval Pacific herring (*Clupea pallasi*). Environ. Toxicol. Chem. 18, 481–493.

Claireaux, G., Davoodi, F., 2010. Effect of exposure to petroleum hydrocarbons upon cardio-respiratory function in the common sole (*Solea solea*). Aquat. Toxicol. 98, 113–119. https://doi.org/10.1016/j.aquatox.2010.02.006.

Claireaux, G., Desaunay, Y., Akcha, F., Auperin, B., Bocquene, G., Budzinkski, H., Cravedi, J., Davoodi, F., Galois, R., Gilliers, C., Goanvec, C., Guerault, D., Imbert, N., Mazeas, O., Nonnotte, G., Nonnotte, L., Prunet, P., Sebert, P., Vettier, A., 2004. Influence of oil exposure on the physiology and ecology of the common sole Solea solea: experimental and field approaches. Aquat. Living Resour. 17, 335–351.

Claireaux, G., Théron, M., Prineau, M., Dussauze, M., Merlin, F.-X., Le Floch, S., 2013. Effects of oil exposure and dispersant use upon environmental adaptation performance and fitness in the European sea bass, *Dicentrarchus labrax*. Aquat. Toxicol. 130 (131), 160–170. https://doi.org/10.1016/j.aquatox.2013.01.004.

Clark, B.W., Bone, A.J., Di Giulio, R.T., 2014. Resistance to teratogenesis by F1 and F2 embryos of PAH-adapted *Fundulus heteroclitus* is strongly inherited despite reduced recalcitrance of the AHR pathway. Environ. Sci. Pollut. Res. Int. 21, 13898–13908. https://doi.org/10.1007/s11356-013-2446-7.

Couillard, C.M., 2002. A microscale test to measure petroleum oil toxicity to mummichog embryos. Environ. Toxicol. 17, 195–202. https://doi.org/10.1002/tox.10049.

Cox, G.K., Crossley, D.A., Stieglitz, J.D., Heuer, R.M., Benetti, D.D., Grosell, M., 2017. Oil exposure impairs in situ cardiac function in response to β-adrenergic stimulation in cobia (*Rachycentron canadum*). Environ. Sci. Technol. 51, 14390–14396. https://doi.org/10.1021/acs.est.7b03820.

Author's personal copy

Cypher, A.D., Consiglio, J., Bagatto, B., 2017. Hypoxia exacerbates the cardiotoxic effect of the polycyclic aromatic hydrocarbon, phenanthrene in *Danio rerio*. Chemosphere 183, 574–581. https://doi.org/10.1016/j.chemosphere.2017.05.109.

de Soysa, T.Y., Ulrich, A., Friedrich, T., Pite, D., Compton, S.L., Ok, D., Bernardos, R.L., Downes, G.B., Hsieh, S., Stein, R., Lagdameo, M.C., Halvorsen, K., Kesich, L.R., Barresi, M.J., 2012. Macondo crude oil from the Deepwater Horizon oil spill disrupts specific developmental processes during zebrafish embryogenesis. BMC Biol. 10, 40. https://doi.org/10.1186/1741-7007-10-40.

Denison, M.S., Nagy, S.R., 2003. Activation of the aryl hydrocarbon receptor by structurally diverse exogenous and endogenous chemicals. Annu. Rev. Pharmacol. Toxicol. 43, 309–334. https://doi.org/10.1146/annurev.pharmtox.43.100901.135828.

Di Toro, D.M., McGrath, J.A., 2000. Technical basis for narcotic chemicals and polycyclic aromatic hydrocarbon criteria. II. Mixtures and sediments. Environ. Toxicol. Chem. 19, 1971–1982. https://doi.org/10.1002/etc.5620190804.

Di Toro, D.M., McGrath, J.A., Stubblefield, W.A., 2007. Predicting the toxicity of neat and weathered crude oil: toxic potential and the toxicity of saturated mixtures. Environ. Toxicol. Chem. 26, 24–36. https://doi.org/10.1897/06174R.1.

Diamante, G., Xu, E.G., Chen, S., Mager, E., Grosell, M., Schlenk, D., 2017. Differential expression of microRNAs in embryos and larvae of mahi-mahi (*Coryphaena hippurus*) exposed to Deepwater Horizon Oil. Environ. Sci. Technol. Lett. 4, 523–529.

Dubansky, B., Whitehead, A., Miller, J.T., Rice, C.D., Galvez, F., 2013. Multitissue molecular, genomic, and developmental effects of the deepwater horizon oil spill on resident Gulf Killifish (*Fundulus grandis*). Environ. Sci. Technol. 47, 5074–5082. https://doi.org/10.1021/es400458p.

Dussauze, M., Camus, L., Le Floch, S., Pichavant-Rafini, K., Geraudie, P., Coquille, N., Amerand, A., Lemaire, P., Theron, M., 2014. Impact of dispersed fuel oil on cardiac mitochondrial function in polar cod *Boreogadus saida*. Environ. Sci. Pollut. Res. Int. 21, 13779–13788. https://doi.org/10.1007/s11356-014-2618-0.

Eckle, P., Burgherr, P., Michaux, E., 2012. Risk of large oil spills: a statistical analysis in the aftermath of Deepwater Horizon. Environ. Sci. Technol. 46, 13002–13008. https://doi.org/10.1021/es3029523.

Edmunds, R.C., Gill, J., Baldwin, D.H., Linbo, T.L., French, B.L., Brown, T.L., Esbaugh, A.J., Mager, E.M., Stieglitz, J., Hoenig, R., others, 2015. Corresponding morphological and molecular indicators of crude oil toxicity to the developing hearts of mahi mahi. Sci. Rep. 5, 1–18.

Esbaugh, A.J., Mager, E.M., Stieglitz, J.D., Hoenig, R., Brown, T.L., French, B.L., Linbo, T.L., Lay, C., Forth, H., Scholz, N.L., Incardona, J.P., Morris, J.M., Benetti, D.D., Grosell, M., 2016. The effects of weathering and chemical dispersion on Deepwater Horizon crude oil toxicity to mahi-mahi (*Coryphaena hippurus*) early life stages. Sci. Total Environ. 543, 644–651. https://doi.org/10.1016/j.scitotenv.2015.11.068.

Farrell, A.P., Eliason, E.J., Sandblom, E., Clark, T.D., 2009. Fish cardiorespiratory physiology in an era of climate change. Can. J. Zool. 87, 835–851. https://doi.org/10.1139/Z09-092.

Farrington, J.W., Quinn, J.G., 2015. "Unresolved Complex Mixture" (UCM): a brief history of the term and moving beyond it. Mar. Pollut. Bull. 96, 29–31. https://doi.org/10.1016/j.marpolbul.2015.04.039.

Gardner, L.D., Peck, K.A., Goetz, G.W., Linbo, T.L., Cameron, J.R., Scholz, N.L., Block, B.A., Incardona, J.P., 2019. Cardiac remodeling in response to embryonic crude oil exposure involves unconventional NKX family members and innate immunity genes. J. Exp. Biol. 222, jeb205567. https://doi.org/10.1242/jeb.205567.

Gerger, C.J., Weber, L.P., 2015. Comparison of the acute effects of benzo-a-pyrene on adult zebrafish (*Danio rerio*) cardiorespiratory function following intraperitoneal injection versus aqueous exposure. Aquat. Toxicol. 165, 19–30.

Greer, J.B., Pasparakis, C., Stieglitz, J.D., Benetti, D., Grosell, M., Schlenk, D., 2019. Effects of corexit 9500A and Corexit-crude oil mixtures on transcriptomic pathways and developmental toxicity in early life stage mahi-mahi (*Coryphaena hippurus*). Aquat. Toxicol. 212, 233–240. https://doi.org/10.1016/j.aquatox.2019.05.014.

Hansen, B.H., Farkas, J., Nordtug, T., Altin, D., Brakstad, O.G., 2018. Does microbial biodegradation of water-soluble components of oil reduce the toxicity to early life stages of fish? Environ. Sci. Technol. 52, 4358–4366. https://doi.org/10.1021/acs.est.7b06408.

Harding, L.B., Tagal, M., Ylitalo, G.M., Incardona, J.P., Davis, J.W., Scholz, N.L., McIntyre, J.K., 2020. Urban stormwater and crude oil injury pathways converge on the developing heart of a shore-spawning marine forage fish. Aquat. Toxicol. 229, 105654. https://doi.org/10.1016/j.aquatox.2020.105654.

Heuer, R.M., Galli, G.L., Shiels, H.A., Fieber, L.A., Cox, G.K., Mager, E.M., Stieglitz, J.D., Benetti, D.D., Grosell, M., Crossley II, D.A., 2019. Impacts of deepwater horizon crude oil on mahi-mahi (*Coryphaena hippurus*) heart cell function. Environ. Sci. Technol. 53, 9895–9904.

Hicken, C.E., Linbo, T.L., Baldwin, D.H., Willis, M.L., Myers, M.S., Holland, L., Larsen, M., Stekoll, M.S., Rice, S.D., Collier, T.K., Scholz, N.L., Incardona, J.P., 2011. Sublethal exposure to crude oil during embryonic development alters cardiac morphology and reduces aerobic capacity in adult fish. Proc. Natl. Acad. Sci. U. S. A. 108, 7086–7090. https://doi.org/10.1073/pnas.1019031108.

Hodson, P.V., 2017. The toxicity to fish embryos of PAH in crude and refined oils. Arch. Environ. Contam. Toxicol. 73, 12–18. https://doi.org/10.1007/s00244-016-0357-6.

Incardona, J., 2017. Molecular mechanisms of crude oil developmental toxicity in fish. Arch. Environ. Contam. Toxicol. 73, 19–32. https://doi.org/10.1007/s00244-017-0381-1.

Incardona, J.P., Carls, M.G., Day, H.L., Sloan, C.A., Bolton, J.L., Collier, T.K., Scholz, N.L., 2009. Cardiac arrhythmia is the primary response of embryonic Pacific herring (Clupea pallasi) exposed to crude oil during weathering. Environ. Sci. Technol. 43, 201–207.

Incardona, J.P., Carls, M.G., Holland, L., Linbo, T.L., Baldwin, D.H., Myers, M.S., Peck, K.A., Tagal, M., Rice, S.D., Scholz, N.L., 2015. Very low embryonic crude oil exposures cause lasting cardiac defects in salmon and herring. Sci. Rep. 5. https://doi.org/10.1038/srep13499.

Incardona, J.P., Carls, M.G., Teraoka, H., Sloan, C.A., Collier, T.K., Scholz, N.L., 2005. Aryl hydrocarbon receptor-independent toxicity of weathered crude oil during fish development. Environ. Health Perspect. 113, 1755–1762.

Incardona, J.P., Collier, T.K., Scholz, N.L., 2004. Defects in cardiac function precede morphological abnormalities in fish embryos exposed to polycyclic aromatic hydrocarbons. Toxicol. Appl. Pharmacol. 196, 191–205. https://doi.org/10.1016/j.taap.2003.11.026.

Incardona, J.P., Gardner, L.D., Linbo, T.L., Brown, T.L., Esbaugh, A.J., Mager, E.M., Stieglitz, J.D., French, B.L., Labenia, J.S., Laetz, C.A., Tagal, M., Sloan, C.A., Elizur, A., Benetti, D.D., Grosell, M., Block, B.A., Scholz, N.L., 2014. Deepwater Horizon crude oil impacts the developing hearts of large predatory pelagic fish. Proc. Natl. Acad. Sci. U. S. A. 111 (15).

Incardona, J.P., Linbo, T.L., French, B.L., Cameron, J., Peck, K.A., Laetz, C.A., Hicks, M.B., Hutchinson, G., Allan, S.E., Boyd, D.T., Ylitalo, G.M., Scholz, N.L., 2021. Low-level embryonic crude oil exposure disrupts ventricular ballooning and subsequent trabeculation in Pacific herring. Aquat. Toxicol. 235, 105810. https://doi.org/10.1016/j.aquatox.2021.105810.

Incardona, J.P., Swarts, T.L., Edmunds, R.C, Linbo, T.L., Aquilina-Beck, A., Sloan, C.A., Gardner, L.D., Block, B.A., Scholz, N.L., 2013. Exxon Valdez to Deepwater Horizon: comparable toxicity of both crude oils to fish early life stages. Aquat. Toxicol. 142-143, 303–316. https://doi.org/10.1016/j.aquatox.2013.08.011.

Incardona, J.P., Scholz, N.L., 2016. The influence of heart developmental anatomy on cardiotoxicity-based adverse outcome pathways in fish. Aquat. Toxicol. 177, 515–525. https://doi.org/10.1016/j.aquatox.2016.06.016.

Jayasundara, N., Van Tiem Garner, L., Meyer, J.N., Erwin, K.N., Di Giulio, R.T., 2015. AHR2-Mediated transcriptomic responses underlying the synergistic cardiac developmental toxicity of PAHs. Toxicol. Sci. 143, 469–481. https://doi.org/10.1093/toxsci/kfu245.

Johansen, J.L., Esbaugh, A.J., 2019. Oil-induced responses of cardiac and red muscle mitochondria in red drum (*Sciaenops ocellatus*). Comp. Biochem. Physiol. C Toxicol. Pharmacol. 219, 35–41. https://doi.org/10.1016/j.cbpc.2019.02.003.

Johansen, J.L., Esbaugh, A.J., 2017. Sustained impairment of respiratory function and swim performance following acute oil exposure in a coastal marine fish. Aquat. Toxicol. 187, 82–89. https://doi.org/10.1016/j.aquatox.2017.04.002.

Jung, J.-H., Hicken, C.E., Boyd, D., Anulacion, B.F., Carls, M.G., Shim, W.J., Incardona, J.P., 2013. Geologically distinct crude oils cause a common cardiotoxicity syndrome in developing zebrafish. Chemosphere 91, 1146–1155. https://doi.org/10.1016/j.chemosphere.2013.01.019.

Jung, J.-H., Kim, M., Yim, U.H., Ha, S.Y., Shim, W.J., Chae, Y.S., Kim, H., Incardona, J.P., Linbo, T.L., Kwon, J.-H., 2015. Differential toxicokinetics determines the sensitivity of two marine embryonic fish exposed to Iranian heavy crude oil. Environ. Sci. Technol. 49, 13639–13648. https://doi.org/10.1021/acs.est.5b03729.

Author's personal copy

Jung, J.-H., Ko, J., Lee, E.-H., Choi, K.-M., Kim, M., Yim, U.H., Lee, J.-S., Shim, W.J., 2017. RNA seq- and DEG-based comparison of developmental toxicity in fish embryos of two species exposed to Iranian heavy crude oil. Comp. Biochem. Physiol. C Toxicol. Pharmacol. 196, 1–10. https://doi.org/10.1016/j.cbpc.2017.02.010.

Jutfelt, F., Norin, T., Ern, R., Overgaard, J., Wang, T., McKenzie, D.J., Lefevre, S., Nilsson, G.E., Metcalfe, N.B., Hickey, A.J.R., Brijs, J., Speers-Roesch, B., Roche, D.G., Gamperl, A.K., Raby, G.D., Morgan, R., Esbaugh, A.J., Gräns, A., Axelsson, M., Ekström, A., Sandblom, E., Binning, S.A., Hicks, J.W., Seebacher, F., Jørgensen, C., Killen, S.S., Schulte, P.M., Clark, T.D., 2018. Oxygen- and capacity-limited thermal tolerance: blurring ecology and physiology. J. Exp. Biol. 221, jeb169615. https://doi.org/10.1242/jeb.169615.

Kennedy, C.J., Farrell, A.P., 2006. Effects of exposure to the water-soluble fraction of crude oil on the swimming performance and the metabolic and ionic recovery postexercise in Pacific herring (*Clupea pallasi*). Environ. Toxicol. Chem. 25, 2715–2724. https://doi.org/10.1897/05-504r.1.

Khursigara, A.J., Ackerly, K.L., Esbaugh, A.J., 2019. Oil toxicity and implications for environmental tolerance in fish. Comp. Biochem. Physiol. C Toxicol. Pharmacol. 220, 52–61. https://doi.org/10.1016/j.cbpc.2019.03.003.

Khursigara, A.J., Perrichon, P., Martinez Bautista, N., Burggren, W.W., Esbaugh, A.J., 2017. Cardiac function and survival are affected by crude oil in larval red drum, *Sciaenops ocellatus*. Sci. Total Environ. 579, 797–804. https://doi.org/10.1016/j.scitotenv.2016.11.026.

Kirby, A.R., Cox, G.K., Nelson, D., Heuer, R.M., Stieglitz, J.D., Benetti, D.D., Grosell, M., Crossley, D.A., 2019. Acute crude oil exposure alters mitochondrial function and ADP affinity in cardiac muscle fibers of young adult Mahi-mahi (*Coryphaena hippurus*). Comp. Biochem. Physiol. C Toxicol. Pharmacol. 218, 88–95. https://doi.org/10.1016/j.cbpc.2019.01.004.

Köhle, C., Bock, K.W., 2007. Coordinate regulation of Phase I and II xenobiotic metabolisms by the Ah receptor and Nrf2. Biochem. Pharmacol. 73, 1853–1862. https://doi.org/10.1016/j.bcp.2007.01.009.

Laurel, B.J., Copeman, L.A., Iseri, P., Spencer, M.L., Hutchinson, G., Nordtug, T., Donald, C.E., Meier, S., Allan, S.E., Boyd, D.T., Ylitalo, G.M., Cameron, J.R., French, B.L., Linbo, T.L., Scholz, N.L., Incardona, J.P., 2019. Embryonic crude oil exposure impairs growth and lipid allocation in a Keystone Arctic forage fish. iScience 19, 1101–1113. https://doi.org/10.1016/j.isci.2019.08.051.

Li, R., Zuo, Z., Chen, D., He, C., Chen, R., Chen, Y., Wang, C., 2011. Inhibition by polycyclic aromatic hydrocarbons of ATPase activities in *Sebastiscus marmoratus* larvae:Relationship with the development of early life stages. Mar. Environ. Res. 71, 86–90. https://doi.org/10.1016/j.marenvres.2010.11.002.

Mager, E.M., Esbaugh, A.J., Stieglitz, J.D., Hoenig, R., Bodinier, C., Incardona, J.P., Scholz, N.L., Benetti, D.D., Grosell, M., 2014. Acute embryonic or juvenile exposure to Deepwater Horizon crude oil impairs the swimming performance of mahi-mahi (*Coryphaena hippurus*). Environ. Sci. Technol. 48, 7053–7061. https://doi.org/10.1021/es501628k.

Mager, E.M., Pasparakis, C., Schlenker, L.S., Yao, Z., Bodinier, C., Stieglitz, J.D., Hoenig, R., Morris, J.M., Benetti, D.D., Grosell, M., 2017. Assessment of early life stage mahi-mahi windows of sensitivity during acute exposures to Deepwater Horizon crude oil. Environ. Toxicol. Chem. https://doi.org/10.1002/etc.3713.

Mager, E.M., Pasparakis, C., Stieglitz, J.D., Hoenig, R., Morris, J.M., Benetti, D.D., Grosell, M., 2018. Combined effects of hypoxia or elevated temperature and Deepwater Horizon crude oil exposure on juvenile mahi-mahi swimming performance. Mar. Environ. Res. 139, 129–135.

Magnuson, J.T., Bautista, N.M., Lucero, J., Lund, A.K., Xu, E.G., Schlenk, D., Burggren, W.W., Roberts, A.P., 2020. Exposure to crude oil induces retinal apoptosis and impairs visual function in fish. Environ. Sci. Technol. 54, 2843–2850. https://doi.org/10.1021/acs.est.9b07658.

Marty, G.D., Hinton, D.E., Short, J.W., Heintz, R.A., Rice, S.D., Dambach, D.M., Willits, N.H., Stegeman, J.J., 1997a. Ascites, premature emergence, increased gonadal cell apoptosis, and cytochrome P4501A induction in pink salmon larvae continuously exposed to oil-contaminated gravel during development. Can. J. Zool. 75, 989–1007.

Marty, G.D., Hose, J.E., McGurk, M.D., Brown, E.D., Hinton, D.E., 1997b. Histopathology and cytogenetic evaluation of Pacific herring larvae exposed to petroleum hydrocarbons in the laboratory or in Prince William sound, Alaska, after the Exxon Valdez oil spill. Can. J. Fish. Aquat. Sci. 54, 1846–1857. https://doi.org/10.1139/f97-091.

Mauduit, F., Domenici, P., Farrell, A.P., Lacroix, C., Le Floch, S., Lemaire, P., Nicolas-Kopec, A., Whittington, M., Zambonino-Infante, J.L., Claireaux, G., 2016. Assessing chronic fish health: an application to a case of an acute exposure to chemically treated crude oil. Aquat. Toxicol. 178, 197–208. https://doi.org/10.1016/j.aquatox.2016.07.019.

Mauduit, F., Farrell, A.P., Domenici, P., Lacroix, C., Le Floch, S., Lemaire, P., Nicolas-Kopec, A., Whittington, M., Le Bayon, N., Zambonino-Infante, J.-L., Claireaux, G., 2019. Assessing the long-term effect of exposure to dispersant-treated oil on fish health using hypoxia tolerance and temperature susceptibility as ecologically relevant biomarkers. Environ. Toxicol. Chem. 38, 210–221. https://doi.org/10.1002/etc.4271.

McGrath, J.A., Fanelli, C.J., Di Toro, D.M., Parkerton, T.F., Redman, A.D., Paumen, M.L., Comber, M., Eadsforth, C.V., den Haan, K., 2018. Re-evaluation of target lipid model–derived HC5 predictions for hydrocarbons. Environ. Toxicol. Chem. 37, 1579–1593. https://doi.org/10.1002/etc.4100.

McIntosh, S., King, T., Wu, D., Hodson, P.V., 2010. Toxicity of dispersed weathered crude oil to early life stages of Atlantic herring (*Clupea harengus*). Environ. Toxicol. Chem. 29, 1160–1167. https://doi.org/10.1002/etc.134.

Meador, J.P., 2021. The fish early-life stage sublethal toxicity syndrome — a high-dose baseline toxicity response. Environ. Pollut., 118201 https://doi.org/10.1016/j.envpol.2021.118201.

Meador, J.P., Nahrgang, J., 2019. Characterizing crude oil toxicity to early-life stage fish based on a complex mixture: are we making unsupported assumptions? Environ. Sci. Technol. 53, 11080–11092. https://doi.org/10.1021/acs.est.9b02889.

Middaugh, D.P., Chapman, P.J., Shelton, M.E., McKenney Jr., C.L., Courtney, L.A., 2002. Effects of fractions from biodegraded Alaska North Slope crude oil on embryonic Inland Silversides, *Menidia beryllina*. Arch. Environ. Contam. Toxicol. 42, 236–243. https://doi.org/10.1007/s00244-001-0006-5.

Milinkovitch, T., Lucas, J., Le Floch, S., Thomas-Guyon, H., Lefrancois, C., 2012. Effect of dispersed crude oil exposure upon the aerobic metabolic scope in juvenile golden grey mullet (*Liza aurata*). Mar. Pollut. Bull. 64, 865–871.

Milinkovitch, T., Thomas-Guyon, H., Lefrancois, C., Imbert, N., 2013. Dispersant use as a response to oil spills: toxicological effects on fish cardiac performance. Fish Physiol. Biochem. 39, 257–262.

Morris, J.M., Gielazyn, M., Krasnec, M.O., Takeshita, R., Forth, H.P., Labenia, J.S., Linbo, T.L., French, B.L., Gill, J.A., Baldwin, D.H., Scholz, N.L., Incardona, J.P., 2018. Crude oil cardiotoxicity to red drum embryos is independent of oil dispersion energy. Chemosphere 213, 205–214. https://doi.org/10.1016/j.chemosphere.2018.09.015.

Mu, J., Chernick, M., Dong, W., Di Giulio, R.T., Hinton, D.E., 2017. Early life co-exposures to a real-world PAH mixture and hypoxia result in later life and next generation consequences in medaka (*Oryzias latipes*). Aquat. Toxicol. 190, 162–173. https://doi.org/10.1016/j.aquatox.2017.06.026.

Mulero-Navarro, S., Fernandez-Salguero, P.M., 2016. New trends in aryl hydrocarbon receptor biology. Front. Cell Dev. Biol. 4.

National Research Council (US) Committee on Oil in the Sea: Inputs, Fates, and Effects, 2003. Oil in the Sea III: Inputs, Fates, and Effects. National Academies Press (US), Washington (DC).

Nelson, D., Heuer, R.M., Cox, G.K., Stieglitz, J.D., Hoenig, R., Mager, E.M., Benetti, D.D., Grosell, M., Crossley, D.A., 2016. Effects of crude oil on in situ cardiac function in young adult mahi–mahi (*Coryphaena hippurus*). Aquat. Toxicol. 180, 274–281. https://doi.org/10.1016/j.aquatox.2016.10.012.

Nelson, D., Stieglitz, J.D., Cox, G.K., Heuer, R.M., Benetti, D.D., Grosell, M., Crossley, D.A., 2017. Cardio-respiratory function during exercise in the cobia, *Rachycentron canadum*: the impact of crude oil exposure. Comp. Biochem. Physiol. C Toxicol. Pharmacol. 201, 58–65. https://doi.org/10.1016/j.cbpc.2017.08.006.

Pan, Y.K., Khursigara, A.J., Johansen, J.L., Esbaugh, A.J., 2018. The effects of oil induced respiratory impairment on two indices of hypoxia tolerance in Atlantic croaker (*Micropogonias undulatus*). Chemosphere 200, 143–150. https://doi.org/10.1016/j.chemosphere.2018.02.028.

Parrott, J.L., Marentette, J.R., Hewitt, L.M., McMaster, M.E., Gillis, P.L., Norwood, W.P., Kirk, J.L., Peru, K.M., Headley, J.V., Wang, Z., Yang, C., Frank, R.A., 2018. Meltwater from snow contaminated by oil sands emissions is toxic to larval fish, but not spring river water. Sci. Total Environ. 625, 264–274. https://doi.org/10.1016/j.scitotenv.2017.12.284.

Pasparakis, C., Mager, E.M., Stieglitz, J.D., Benetti, D., Grosell, M., 2016. Effects of Deepwater Horizon crude oil exposure, temperature and developmental stage on oxygen consumption of embryonic and larval mahi-mahi (*Coryphaena hippurus*). Aquat. Toxicol. 181, 113–123.

Perrichon, P., Mager, E.M., Pasparakis, C., Stieglitz, J.D., Benetti, D.D., Grosell, M., Burggren, W.W., 2018. Combined effects of elevated temperature and Deepwater Horizon oil exposure on the cardiac performance of larval mahi-mahi, *Coryphaena hippurus*. PLoS One 13, e0203949.

Author's personal copy

Perrichon, P., Pasparakis, C., Mager, E.M., Stieglitz, J.D., Benetti, D.D., Grosell, M., Burggren, W.W., 2017. Morphology and cardiac physiology are differentially affected by temperature in developing larvae of the marine fish mahi-mahi (*Coryphaena hippurus*). Biol. Open 6, 800–809.

Philibert, D.A., Lyons, D., Philibert, C., Tierney, K.B., 2019. Field-collected crude oil, weathered oil and dispersants differentially affect the early life stages of freshwater and saltwater fishes. Sci. Total Environ. 647, 1148–1157. https://doi.org/10.1016/j.scitotenv.2018.08.052.

Plaut, I., 2001. Critical swimming speed: its ecological relevance. Comp. Biochem. Physiol. Mol. Integr. Physiol. 131, 41–50.

Pollino, C.A., Holdway, D.A., 2002. Toxicity testing of crude oil and related compounds using early life stages of the crimson-spotted rainbowfish (*Melanotaenia fluviatilis*). Ecotoxicol. Environ. Saf. 52, 180–189.

Porrello, E.R., Mahmoud, A.I., Simpson, E., Johnson, B.A., Grinsfelder, D., Canseco, D., Mammen, P.P., Rothermel, B.A., Olson, E.N., Sadek, H.A., 2013. Regulation of neonatal and adult mammalian heart regeneration by the miR-15 family. Proc. Natl. Acad. Sci. U. S. A. 110, 187–192. https://doi.org/10.1073/pnas.1208863110.

Raimondo, S., Jackson, C.R., Krzykwa, J., Hemmer, B.L., Awkerman, J.A., Barron, M.G., 2014. Developmental toxicity of Louisiana crude oil-spiked sediment to zebrafish. Ecotoxicol. Environ. Saf. 108, 265–272.

Reddy, C.M., Arey, J.S., Seewald, J.S., Sylva, S.P., Lemkau, K.L., Nelson, R.K., Carmichael, C.A., McIntyre, C.P., Fenwick, J., Ventura, G.T., Van Mooy, B.A., Camilli, R., 2012. Composition and fate of gas and oil released to the water column during the Deepwater Horizon oil spill. Proc. Natl. Acad. Sci. U. S. A. 109, 20229–20234. https://doi.org/10.1073/pnas.1101242108.

Rhodes, S., Farwell, A., Mark Hewitt, L., MacKinnon, M., George Dixon, D., 2005. The effects of dimethylated and alkylated polycyclic aromatic hydrocarbons on the embryonic development of the Japanese medaka. Ecotoxicol. Environ. Saf. 60, 247–258. https://doi.org/10.1016/j.ecoenv.2004.08.002.

Scott, J.A., Incardona, J.P., Pelkki, K., Shepardson, S., Hodson, P.V., 2011. AhR2-mediated, CYP1A-independent cardiovascular toxicity in zebrafish (*Danio rerio*) embryos exposed to retene. Aquat. Toxicol. 101, 165–174. https://doi.org/10.1016/j.aquatox.2010.09.016.

Sikkema, J., de Bont, J.A., Poolman, B., 1995. Mechanisms of membrane toxicity of hydrocarbons. Microbiol. Rev. 59, 201–222.

Sørhus, E., Incardona, J.P., Furmanek, T., Goetz, G.W., Scholz, N.L., Meier, S., Edvardsen, R.B., Jentoft, S., 2017. Novel adverse outcome pathways revealed by chemical genetics in a developing marine fish. elife 6, e20707. https://doi.org/10.7554/eLife.20707.

Sørhus, E., Incardona, J.P., Karlsen, Ø., Linbo, T., Sørensen, L., Nordtug, T., van der Meeren, T., Thorsen, A., Thorbjørnsen, M., Jentoft, S., Edvardsen, R.B., Meier, S., 2016. Crude oil exposures reveal roles for intracellular calcium cycling in haddock craniofacial and cardiac development. Sci. Rep. 6, 31058. https://doi.org/10.1038/srep31058.

Spitsbergen, J.M., Walker, M.K., Olson, J.R., Peterson, R.E., 1991. Pathologic alterations in early life stages of lake trout, *Salvelinus namaycush*, exposed to 2,3,7,8-tetrachlorodibenzo- p-dioxin as. Aquat. Toxicol. 19, 41–71. https://doi.org/10.1016/0166-445X(91)90027-7.

Stanfel, M.N., Moses, K.A., Schwartz, R.J., Zimmer, W.E., 2005. Regulation of organ development by the NKX-homeodomain factors: an NKX code. Cell Mol. Biol. (Suppl. 51), OL785–799.

Staudt, D.W., Liu, J., Thorn, K.S., Stuurman, N., Liebling, M., Stainier, D.Y.R., 2014. High-resolution imaging of cardiomyocyte behavior reveals two distinct steps in ventricular trabeculation. Development 141, 585–593. https://doi.org/10.1242/dev.098632.

Sun, B., Huo, R., Sheng, Y., Li, Y., Xie, X., Chen, C., Liu, H.-B., Li, N., Li, C.-B., Guo, W.-T., Zhu, J.-X., Yang, B.-F., Dong, D.-L., 2013. Bone morphogenetic protein-4 mediates cardiac hypertrophy, apoptosis, and fibrosis in experimentally pathological cardiac hypertrophy. Hypertension 61, 352–360. https://doi.org/10.1161/HYPERTENSIONAHA.111.00562.

Sweet, L.E., Magnuson, J., Garner, T.R., Alloy, M.M., Stieglitz, J.D., Benetti, D., Grosell, M., Roberts, A.P., 2017. Exposure to ultraviolet radiation late in development increases the toxicity of oil to mahi-mahi (*Coryphaena hippurus*) embryos. Environ. Toxicol. Chem. 36, 1592–1598. https://doi.org/10.1002/etc.3687.

Sweet, L.E., Revill, A.T., Strzelecki, J., Hook, S.E., Morris, J.M., Roberts, A.P., 2018. Photo-induced toxicity following exposure to crude oil and ultraviolet radiation in 2 Australian fishes. Environ. Toxicol. Chem. 37, 1359–1366. https://doi.org/10.1002/etc.4083.

Vehniäinen, E.-R., Haverinen, J., Vornanen, M., 2019. Polycyclic aromatic hydrocarbons phenanthrene and retene modify the action potential via multiple ion currents in rainbow trout *Oncorhynchus mykiss* cardiac myocytes. Environ. Toxicol. Chem. 38, 2145–2153. https://doi.org/10.1002/etc.4530.

Xu, E.G., Khursigara, A.J., Magnuson, J., Hazard, E.S., Hardiman, G., Esbaugh, A.J., Roberts, A.P., Schlenk, D., 2017a. Larval red drum (*Sciaenops ocellatus*) sublethal exposure to weathered deepwater horizon crude oil: developmental and transcriptomic consequences. Environ. Sci. Technol. 51, 10162–10172. https://doi.org/10.1021/acs.est.7b02037.

Xu, E.G., Mager, E.M., Grosell, M., Hazard, E.S., Hardiman, G., Schlenk, D., 2017b. Novel transcriptome assembly and comparative toxicity pathway analysis in mahi-mahi (*Coryphaena hippurus*) embryos and larvae exposed to Deepwater Horizon oil. Sci. Rep. 7, 44546.

Xu, E.G., Mager, E.M., Grosell, M., Pasparakis, C., Schlenker, L.S., Stieglitz, J.D., Benetti, D., Hazard, E.S., Courtney, S.M., Diamante, G., others, 2016. Time-and oil-dependent transcriptomic and physiological responses to Deepwater Horizon oil in mahi-mahi (*Coryphaena hippurus*) embryos and larvae. Environ. Sci. Technol. 50, 7842–7851.

Xu, E.G., Magnuson, J.T., Diamante, G., Mager, E., Pasparakis, C., Grosell, M., Roberts, A.P., Schlenk, D., 2018. Changes in microRNA–mRNA signatures agree with morphological, physiological, and behavioral changes in larval mahi-mahi treated with Deepwater Horizon oil. Environ. Sci. Technol. 52, 13501–13510.

Zhang, Y., Huang, L., Wang, C., Gao, D., Zuo, Z., 2013. Phenanthrene exposure produces cardiac defects during embryo development of zebrafish (*Danio rerio*) through activation of MMP-9. Chemosphere 93, 1168–1175. https://doi.org/10.1016/j.chemosphere.2013.06.056.